# Energy system co-design approach for WECs optimisation: the pendulum wave energy converter case study

Filippo Giorcelli [a,*] ⓘ, Pedro Cabrera [b] ⓘ, Bruno Paduano [a] ⓘ, Sergej Antonello Sirigu [a], Giuliana Mattiazzo [a]

[a] *Marine Offshore Renewable Energy Lab (MOREnergy Lab), Department of Mechanical and Aerospace Engineering, Politecnico di Torino, Corso Duca degli Abruzzi 24, 10129, Torino, Italy*
[b] *Department of Mechanical Engineering, University of Las Palmas de Gran Canaria, Campus de Tafira S/N, 35017, Las Palmas de Gran Canaria, Canary Islands, Spain*

## HIGHLIGHTS

- Co-design framework couples WEC design with energy system planning.
- Multi-objective optimisation reduces $CO_2$ and renewable energy mismatch.
- Optimal WECs designs enhance system-level performance, not just device-level ones.
- The co-design method applied to La Gomera achieves 50 % $CO_2$ cut and 90 % RES share.
- The energy system co-design method is applicable to other systems and technologies.

## ARTICLE INFO

## ABSTRACT

The integration of wave energy into power systems is often hindered by a mismatch between device-level performance and system-level. Conventional early-stage Wave Energy Converters (WECs) design frameworks, typically guided by levelised cost of energy minimisation, overlook systemic benefits such as aligning renewable production with the system's demand. This paper proposes a co-design framework that simultaneously optimises WEC design and the renewable energy mix, ensuring that the selected design performs optimally within the overall system while embedding the system's constraints and performance targets into early-stage WEC design. The approach is demonstrated for the Pendulum WEC (PeWEC) within La Gomera's isolated grid, in the Canary archipelago, a relevant testbed for microgrid decarbonisation. A multi-objective genetic algorithm couples the PeWEC numerical model with the EnergyPLAN simulation tool to perform hourly-based annual simulations of the whole energy system. The framework identifies Pareto-optimal solutions that reduce $CO_2$ emissions and curtailment, reaching up to 50 % $CO_2$ reduction and 90 % renewable energy sources (RES) share. Results show that optimal devices are not those with maximum stand-alone productivity but those providing power profiles that stabilise the grid and improve RES integration. The methodology enables a comprehensive assessment of wave energy value by embedding system-level constraints directly into the design process and provides practical evidence of how wave energy can support the decarbonisation of isolated grids. The approach is generalisable to other remote, hybrid, or high-RES systems and RES technologies.

## 1. Introduction

Acknowledging the pressing need for climate action, the European Union (EU) governments have set forth an ambitious agenda to achieve carbon neutrality and establish a fully decarbonised energy system. The EU vision is articulated in what has been referred to as "*the most ambitious EU research and innovation programme ever*" [1]. In the transition towards a sustainable energy system, the replacement of fossil-based systems with renewable energy sources (RES) presents a wide consensus

---

## Nomenclature

*Acronyms*

| | |
|---|---|
| AEP | Annual Energy Production |
| BEM | Boundary Element Method |
| BESS | Battery Energy Storage System |
| BFR | Ballast Filling Ratio |
| CapEx | Capital Expenditure |
| EU | European Union |
| GA | Genetic Algorithm |
| ISTAC | Instituto Canario de Estadistica |
| JONSWAP | JOint North Sea WAve Project |
| LCoE | Levelized Cost of Energy |
| NSGA-II | Non-dominated Sorting Genetic Algorithm II |
| OpEx | Operational Expenditure |
| OWT | Offshore Wind Turbine |
| PeWEC | Pendulum Wave Energy Converter |
| PP | Power Plant |
| PV | Photovoltaic |
| REE | Red Eléctrica de España |
| RES | Renewable Energy Source |
| TRL | Technology Readiness Level |
| TPL | Technology Performance Level |
| TSO | Transmission System Operator |
| WEC | Wave Energy Converter |
| WT | Wind Turbine |

*Variables*

| | |
|---|---|
| $\mathbf{d}$ | Design vector |
| $\mathcal{D}$ | Design space |
| $\mathbf{D_l}$ | Design space lower bound |
| $\mathbf{D_u}$ | Design space upper bound |
| $\mathbf{f(d)}$ | Objective functions vector |
| $\mathbf{g(d)}$ | Sets of inequality constraints |
| $\mathbf{h(d)}$ | Sets of equality constraints |
| $OP_{RES}$ | Annual RES overproduction |
| $CO_2$ | Carbon dioxide |
| $C_{RES_i}$ | Installed capacity for the $i$-th RES |
| $N_{RES}$ | Number of distinct RES integrated into the energy system |
| $N_{WEC}$ | Number of WEC's design parameters |
| $N_y$ | Number of hours in the year |
| $\Psi$ | Ideal storage system size |
| $E_{RES_i}^h$ | Energy produced by the $i$-th RES during hour $h$ |
| $I_+^h$ | Hourly indicator function |
| $E_{RES_i}^h$ | Energy produced by the PP during hour |
| $\mathbf{e}$ | Energy system state vector |
| $\mathbf{w}$ | WEC's design vector |
| $\mathcal{E}$ | Energy system's design space |
| $\mathcal{W}$ | WEC's design space |
| $C_{wave}$ | Wave energy installed capacity |
| $C_{pv}$ | PV installed capacity |
| $C_{wind}$ | Wind turbine installed capacity |
| $C_{owt}$ | Offshore wind turbine installed capacity |
| $C_{PP}$ | Conventional PP installed capacity |
| $C_{BESS}$ | BESS installed energy capacity |
| $\eta_{PP}$ | PP conversion efficiency |
| $N_{gas}$ | Natural gas demand |
| $F_t$ | Fuel consumption for transport sector |
| $D_e$ | Annual electricity demand |
| $D_c$ | Annual cooling demand |

| | |
|---|---|
| $D_h$ | Annual heating demand |
| $\hat{\mathbf{D}}_e$ | Annual electricity demand normalised distribution |
| $\hat{\mathbf{D}}_c$ | Annual cooling demand normalised distribution |
| $\hat{\mathbf{D}}_h$ | Annual heating demand normalised distribution |
| $\hat{\mathbf{P}}_{wind}$ | Annual WT energy production normalised distribution |
| $\hat{\mathbf{P}}_{owt}$ | Annual OWT energy production normalised distribution |
| $\hat{\mathbf{P}}_{pv}$ | Annual PV energy production normalised distribution |
| $\hat{\mathbf{P}}_{wave}$ | Annual WEC energy production normalised distribution |
| $S_{ch}$ | Storage charge capacity |
| $S_{dis}$ | Storage discharge capacity |
| $\eta_{ch}$ | Storage charge efficiency |
| $\eta_{ch}$ | Storage charge efficiency |
| $\eta_{dis}$ | Storage discharge efficiency |
| $P_{WEC}$ | WEC's mean absorbed power |
| $H_s$ | Significant wave height |
| $T_e$ | Energetic wave period |
| $\mathbf{u}$ | WEC's state of motion vector |
| $x$ | Surge |
| $z$ | Heave |
| $\delta$ | Pitch |
| $\varepsilon$ | Pendulum oscillation |
| $\mathbf{M}$ | Mass matrix |
| $\mathbf{A}(\omega)$ | Added mass |
| $\mathbf{B}(\omega)$ | Radiation damping |
| $\mathbf{F}_\omega(\omega)$ | Waves' excitation coefficients |
| $\omega$ | Frequencies |
| $\mathbf{K}_h$ | Hydrostatic stiffness matrix |
| $\mathbf{K}_p$ | Pendulum restoring force |
| $a_\omega(\omega)$ | Wave amplitude |
| $h$ | $\mathbf{T}_{PTO}$ PTO torque |
| $m_h$ | Hull mass |
| $m_p$ | Pendulum mass |
| $g$ | Gravitational acceleration |
| $I_h$ | Hull moment of inertia |
| $I_p$ | Pendulum moment of inertia |
| $d$ | Distance between WEC's center of gravity and $\varepsilon$-axis |
| $l$ | Pendulum arm length |
| $T_{ctrl}$ | Applied control torque |
| $\tau_{gear}$ | Gearbox ratio |
| $\alpha_{PTO}$ | First control parameter |
| $\beta_{PTO}$ | Second control parameter |
| $S_{\dot{\varepsilon}\dot{\varepsilon}}(\omega)$ | Power spectral density of the $\varepsilon$-axis rotational velocity |
| $N_w$ | Non-zero occurring waves |
| $N_c$ | Number of simulated waves for the control loop |
| $Occ_\%$ | Wave's occurrences in percentage |
| $L$ | Hull length |
| $W$ | Hull width |
| $h$ | Hull shape ratio |
| $k$ | Hull height ratio |
| $\alpha$ | Hull draft parameter |
| $l$ | Pendulum arm length |
| $\phi$ | Pendulum mass width |
| $\zeta$ | Pendulum mass height |
| $N_u$ | Number of pendulum units |
| $\lambda_0$ | Unit position |
| $\rho_h$ | Hull steel density |
| $\rho_p$ | Pendulum mass density |
| $\rho_b$ | Ballast sand density |

and highlights the pivotal role played by RES in such context [2–6]. However, as RES penetration increases, the intermittent nature of these sources calls for robust and accurate energy planning strategies [7–10]. Moreover, given the global scale of the challenge and considering the

Earth's climatic variations, new emerging clean energy technologies and energy system planning strategies should be designed in order to efficiently operate across different environmental conditions.

In this context, RES integration in islands holds a relevant position as a testing ground for the employment of novel decarbonisation strategies, system architectures or technologies [11]. Cross et al. [12] present a literature review on the potential for RES penetration in islands, highlighting that they represent ideal testbeds for pilot projects on emerging energy technologies. This is attributed to their compact scale, power systems where the interaction between producers and end-users is more direct and involves fewer intermediaries, and their cohesive communities. All this facilitates consumer engagement and allows customers to directly perceive the value and effectiveness of the tested energy supply solutions. Accordingly, EU also involves islands in the development of its sustainable transition paths [13–15].

Scenarios for off-grid energy systems sited in remote areas have to be designed not only with the aim to minimising the system cost but also in order to ensure compliance with the network technical operational requirements, *i.e.* maintaining power reserves and balancing the energy grid [7,16]. Therefore, significant challenges arise for high-RES penetration energy systems, especially non-interconnected ones, which is often the case for islands. One of the main issues is the mismatch between the discontinuous energy produced by RES and the actual energy demand of the grid [17,18]. Although storage systems can help to stabilise and synchronise the fluctuating behaviour of RES with the system demand [19,20], oversizing storage systems results in the risk of high costs and low storage efficiency. Therefore, it is essential to diversify installed RES to effectively cope with the grid instability issue and increase the distributed energy system reliability [18].

### 1.1. Wave energy conversion technologies and their integration into energy systems

Besides well-established technologies like photovoltaics (PV) and wind energy, an emerging sector is wave energy. In this area, developers are trying to exploit the very large untapped potential of wave energy [21,22], especially for islands, where the waves' resource is abundant. Among its main advantages, Ringwood [23] highlights its high energy density (over ten times higher than both wind and solar), its availability levels (90 % compared to 20–30 % for wind and solar [24,25]), and its low environmental impact. Moreover, wave energy can help smooth overall power production when combined with other RES [26–29] and can be statistically forecasted 1–2 days in advance [30].

Wave Energy Converters (WECs) are devices designed to harvest wave motion and generate electricity. A generic WEC power train can be divided into four stages: wave absorption, mechanical transmission to the Power Take-Off (PTO), power generation, and power conditioning for grid delivery [31]. Since 1799, a wide variety of wave energy conversion patents have been registered, with remarkable improvement of the technology readiness level (TRL) and the performance level (TPL) over the last decades [32]. Nevertheless, WECs are still at an early stage of development and not yet commercialised. The main barriers to industrialisation are the lack of design convergence, the wide variety of archetypes and operating principles, and the strong dependence on site-specific conditions [23]. For interested readers, comprehensive surveys are provided in [23,32,33].

Early-stage research tends to prioritise technical performance (78 % of studies) over economic (8 %) or techno-economic (14 %) aspects [32]. While many studies focus on maximising annual energy production (AEP), this metric alone is insufficient to ensure economic feasibility. As for other energy technologies, WECs are also evaluated based on their cost of energy, and design optimisation plays a key role in improving both performance and cost-effectiveness [32,34,35]. However, the lack of standardised optimisation methodologies remains a major challenge [32], partly because of the diversity and complexity of WEC designs. Although the levelised cost of energy (LCoE) is a recognised metric, it is seldom used in early-stage design, where alternative indicators such as displaced mass, installed power, or capital expenditure per unit of AEP are often preferred [36–38].

A brief review of the literature reveals that key research directions include geometric optimisation [32,35], manufacturability, and reliability studies [39–41], as well as multidisciplinary approaches combining engineering, economics, and policy [42]. Furthermore, Trueworthy and DuPont [43] underscore the absence of standardised methodologies for assessing WECs' grid integration and call for the development of frameworks that incorporate ancillary benefits beyond conventional metrics such as the LCoE.

Despite these advances, a major gap remains: the lack of energy system-aware WEC design optimisation frameworks. Some recent works, *e.g.* [44], propose optimisation approaches that incorporate wave energy, planning models and system-level metrics (such as avoided costs and environmental externalities [45–47]), but do not evaluate specific WEC designs. Similarly, studies include WECs in hybrid energy systems for isolated grids and consider curtailment, storage, and stability issues [48,49], but do not embed WEC design in scenario-based planning.

### 1.2. Objectives

Despite the growing interest in WECs, their transition from research to deployment remains hindered by several persistent challenges and research gaps. Unlike more mature renewable energy technologies such as PV panels and wind turbines (WTs), WECs are characterised by high design heterogeneity and remain in a pre-commercial stage, with limited consensus on standard evaluation metrics.

A review of the literature reveals a significant gap: while energy system planning models are increasingly used to inform the role of wave energy in future energy mixes, they do not provide feedback to the WEC design process [50–54]. Similarly, most WEC design optimisation studies disregard energy system information, treating the device in isolation. As a result, most WECs' optimisation strategies focus on improving device-level performance without considering how WECs interact with the broader energy system in which they are deployed.

To the best of the authors' knowledge, no existing work formulates an energy-system-informed optimisation framework that directly couples WEC design with energy system dynamics under realistic planning scenarios.

Despite being generally relevant, this limitation is particularly critical for isolated energy systems, such as non-interconnected islands, remote mainland microgrids, hybrid off-grid communities, or weakly supported grids. In these contexts, optimal renewable integration requires a careful alignment between resource availability, system demand and storage needs. Neglecting these interactions in both WEC and energy system's design stages may lead to suboptimal WEC's and system performance.

This paper aims to bridge this gap by proposing a general and modular co-design methodology that simultaneously optimises the design of the WEC system and the configuration of the renewable energy portfolio within the target energy system. The approach is grounded in scenario-based energy planning and explicitly incorporates system-level information, demand profiles, and renewable resource availability. By embedding this data directly into the WEC design optimisation process, the proposed framework enables the joint evaluation of device-level characteristics and their broader impact on energy system performance. This co-design perspective allows for the identification of WEC configurations that not only perform well in isolation, but also enhance the performance of the energy system as a whole.

To verify the effect of the proposed grid-informed design approach, the methodology is applied to a case study involving the island of La Gomera and the Pendulum Wave Energy Converter (PeWEC) device. The local energy system is modelled using EnergyPLAN, a scenario-based simulation tool that captures hourly dynamics of electricity generation, demand, storage, and curtailment. The model is calibrated and validated

using real operational data to ensure realistic representation of system behaviour. Through this application, the paper demonstrates how co-design can inform strategic decisions on WEC sizing and operation that are aligned with system-level planning goals.

A key strength of the proposed methodology lies in its versatility and scalability. While demonstrated in the context of a non-interconnected island, the modular structure and energy-system-aware logic make the framework readily applicable to a wide range of energy system scenarios. Therefore, the proposed methodology serves as a flexible decision-support tool for the broader energy transition, particularly in systems where planning and design must be closely coordinated.

In summary, the main contributions of this work are:

- The formulation of a general, energy-system-informed optimisation framework for WEC design, integrating device and system-level metrics within a unified structure.
- The application of this framework through a representative case study, coupling detailed physical modelling of a WEC with validated energy system simulations.
- The provision of a replicable approach to support decision-making in WEC development that is aligned with real-world energy planning needs, enhancing the viability and strategic deployment of wave energy technologies.

### 1.3. Structure of the manuscript

The remainder of the paper is organised as follows. In Section 2, the overall co-design framework adopted in this study is introduced, outlining the multi-objective optimisation problem formulation. Moreover, in Section 2.1.1, the EnergyPLAN tool and energy system model are presented together with a focus on the framework employed to solve the energy system co-design WEC optimisation. The case study of La Gomera is described in Section 3, including details on the island's current energy system, renewable resource availability, and relevance as a testbed for high-RES scenarios. Furthermore, this section includes a validation of the EnergyPLAN energy system model using real-world data. The same section reports the WEC's governing equations and mathematical model, followed by a description of the design parametrisation employed during the performance evaluation, along with the optimisation. The section also details the algorithm used to identify Pareto-optimal WEC configurations. Section 4 presents a comprehensive analysis of the results, with emphasis on both WEC design trends and impacts on the energy system. Finally, Section 5 provides the main conclusions of the study and outlines possible paths for future investigations.

### 1.4. Notation

The standard notation used throughout this paper is reported in this section. $\mathbb{R}$ denotes the set of real numbers, $\mathbb{C}$ refers to the complex one (with Re referring to the real part and Im to the imaginary one), while the imaginary unit is reported as $j$. Any null element, regardless of its dimension, is reported as 0. A set of positive natural numbers up to $n$, is defined as $\mathbb{N}_n = \{1, 2, \ldots, n\}$. Matrices and vectors are shown as variables in upper and lower case, respectively, both in boldface letters. Then, given a matrix $\mathbf{M} \in \mathbb{R}^{r \times c}$ with $r$ rows and $c$ columns, its $ab$-entry is denoted as $M_{a,b}$ with $a \in \mathbb{N}_r$ and $b \in \mathbb{N}_c$. Similarly, given a vector $\mathbf{v} \in \mathbb{R}^s$ with $s$ elements, its $a$-entry is denoted as $v_a$ with $a \in \mathbb{N}_s$. The transposition operator is denoted as $^T$, while the normalisation of a vector with respect to the maximum among its elements (*e.g.* the peak value of a time series) is defined by $\hat{\ }$.

## 2. Methodology

### 2.1. Energy system co-design framework

As previously outlined, the primary objective of this framework is to identify the optimal energy mix for the analysed energy system, while concurrently refining the design of the considered WEC within such scenarios. Given the significant interactions between the WEC and the
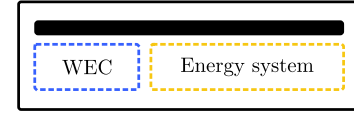


**Fig. 1.** Schematisation of the applied energy system co-design paradigm, adapted from Ringwood [55]. The horizontal black bar shows that WEC and energy system models are jointly optimised.

energy system in which it operates, it is essential that the device design is optimised to ensure suitability and high performance within a specific energy system. Following the approach proposed in [55], this work adopts a simultaneous and co-design philosophy, which is schematically illustrated in Fig. 1.

To this end, the proposed framework is built upon the formulation and resolution of a general optimisation problem, defined as:

$$\min_{\mathbf{d} \in D} \mathbf{f}(\mathbf{d}),$$
$$\text{s.t.}$$
$$\mathbf{g}(\mathbf{d}) \leq 0, \tag{1}$$
$$\mathbf{h}(\mathbf{d}) = 0,$$

where $\mathbf{d}$ represents the overall design vector (obtained by concatenating the WEC design vector with the energy system state vector), $D$ is the design space, $\mathbf{f}(\mathbf{d})$ is the objective function vector, while $\mathbf{g}(\mathbf{d})$ and $\mathbf{h}(\mathbf{d})$ represent the sets of equality and inequality constraints, respectively.

As anticipated in Section 1, one of the strengths of the proposed energy system co-design framework lies in its generality and modular structure. Fundamentally, the framework requires only the mathematical representations of two components: the WEC device and the energy system in which it operates. These models must be parametrised in a way that allows them to interact meaningfully, enabling the formulation of objective functions and constraints that reflect the performance and feasibility of the overall integrated system.

Once a suitable mathematical model for a given WEC is defined, along with a formulation for how it interacts with the surrounding energy system, the same co-design methodology here presented can be extended and applied to any device–system configuration. The structure of the optimisation problem remains unchanged, it is the models and parameter mappings that define its specific application. This flexibility makes the proposed approach highly transferable across different contexts, WEC technologies, and energy system topologies, from standalone island systems to remote microgrids or even interconnected regional networks.

In this study, to suggest the feasibility and effectiveness of the framework, a classic linear frequency-domain model has been employed to represent the WEC dynamics, while the energy system has been modelled using EnergyPLAN, a scenario-based simulation tool widely used for detailed energy system analysis. The energy system model has been validated using real-world operational data to ensure the reliability and credibility of the co-simulation results.

Similarly to [56,57], as system-wide performance metrics, the presented framework proposes the $CO_2$ emissions and the difference between the annual RES overproduction ($OP_{RES}$) and the annual PP production, namely $U_y$. The path to achieving complete carbon neutrality requires a severe reduction of greenhouse gas emissions. Due to this reason, it is straightforward that the motivation behind the choice to set the $CO_2$ emissions as the first framework objective function. Instead, while increasing renewable energy capacity is often seen as a key strategy for reducing reliance on conventional power plants (PP), doing so without consideration of system constraints can lead to inefficiencies. In general, overdimensioning renewable installations purely to cover periods of low resource availability may result in underutilised assets and unnecessary costs. This issue becomes even more critical in small and
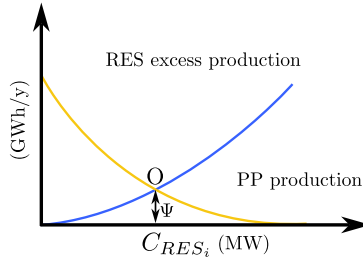
**Fig. 2.** Generalised representation of the defined objective function.

isolated energy systems, where limited space, infrastructure constraints, and higher integration costs make it impractical to rely solely on over-sized renewable capacity to ensure supply continuity in the absence of conventional power sources.

To address this issue, a similar approach to the one presented by Cabrera et al. in [56] has been adopted. With the aim to represent such adopted approach, in Fig. 2 the annual cumulative PP production (yellow line in Fig. 2) and RES excess production trends (blue line in Fig. 2) are represented for a single RES case. In the *x*-axis of the plot, $C_{RES_i}$ denotes the installed capacity for the *i*-th RES, with $i \in \mathbb{N}_{N_{RES}}$ and $N_{RES}$ representing the total number of distinct RES integrated into the energy system. O represents the point of intersection between cumulative RES and PP productions, *i.e.* where the total RES generation matches the annual cumulative demand and making the PP unnecessary under the assumption of ideal storage. As anticipated, the contextual $CO_2$ emissions minimisation is equivalent to reducing the size of such assumed ideal storage system ($\Psi$) when RES excess of production and PP production are equal (*i.e.* the point O).

In the present study we measure the absolute value of the difference between the cumulative RES excess of production, defined as the electricity generated in excess by the RES with respect to the demand, and the annual PP production. This indicator is denoted as $U_y$, and in this work it has been chosen as second system-wide objective function aiming to identify a balanced energy system configuration through the solution of the co-design optimisation problem. Therefore, the mathematical calculation of $U_y$ starts with the evaluation of the annual RES overproduction ($OP_{RES}$):

$$OP_{RES} = \sum_{h=1}^{N_y} \left[ \left[ I_+^h \cdot \sum_{i=1}^{N_{RES}} E_{RES_i}^h \right] - D_e^h \right], \tag{2}$$

in which $E_{RES_i}^h$ and $D_e^h$ denote the energy produced by the *i*-th RES (out of $N_{RES}$ sources) and the electrical demand during hour *h*-th of $N_y$ hours in a year, and where the hourly indicator function $I_+^h$ distinguishes the hours of overproduction and those when the PP needs to be activated:

$$I_+^h = \begin{cases} 1, & \text{if } \sum_{i=1}^{N_{RES}} (E_{RES_i}^h) - D_e^h > 0, \\ 0, & \text{if } \sum_{i=1}^{N_{RES}} (E_{RES_i}^h) - D_e^h \le 0. \end{cases} \tag{3}$$

Then, $U_y$ is evaluated as the absolute value of the difference between the annual RES overproduction $OP_{RES}$ and the annual PP production $\sum_{h=1}^{N_y} E_{PP}^h$:

$$U_y = |OP_{RES} - \sum_{h=1}^{N_y} E_{PP}^h|. \tag{4}$$

In Fig. 2, each point of the blue curve represents the annual RES overproduction $OP_{RES}$, while each point of the yellow curve represents the annual PP production $\sum_{h=1}^{N_y} E_{PP}^h$, as a function of the reference energy

system scenario. In this example, the scenario is described by a single RES technology, whose capacity is progressively varied to span the design space. Reducing $U_y$ to zero (point O, in Fig. 2) would imply an equal amount of annual RES' overproduction for both RES and PP. In such condition, assuming an ideal storage system (of size $\Psi$, in Fig. 2), the PP would no longer be necessary.

Despite referring to the cumulative data is a simplification of real-world, referring to $U_y$ as an additional objective function would help to avoid overdimensioning the size of installed RES capacity while contextually reducing $CO_2$ emissions. Such choice aligns with increasing RES penetration along with reducing their overproduction by matching the hourly system energy demand with RES production. In this way, the optimisation moves towards a scenario where to the installed RES production corresponds to the minimum mismatch with the demand, *i.e.* a balanced energy system. Referring again to Fig. 2, the optimisation problem would tend to reduce $\Psi$, by the translation of point O toward 0 along the *y*-axis (*i.e.* following the reduction of $CO_2$ and therefore of annual PP production), indicating a reduction of the mismatch between annual RES overproduction and PP production.

Therefore, the actual formulation of the optimisation problem for the present investigation is expressed as:

$$\min_{\mathbf{d} \in D} [CO_2(\mathbf{d}), U_y(\mathbf{d})],$$

$$\text{s.t.} \tag{5}$$

$$\mathbf{D}_l \le \mathbf{d} \le \mathbf{D}_u,$$

where the design vector is the concatenation between the energy system state vector $\mathbf{e} \in \mathcal{E} \subset \mathbb{R}^{N_{RES}}$ and the WEC's design vector $\mathbf{w} \in \mathcal{W} \subset \mathbb{R}^{N_{WEC}}$, where $N_{WEC}$ is the number of WEC's design parameters. Namely, the design vector of the entire the energy system co-design optimisation is $\mathbf{d} = \mathbf{w} \parallel \mathbf{e}$ and belongs to the design space $\mathbf{d} \in D \subset \mathbb{R}^{N_{WEC}+N_{RES}}$. Moreover, each element of $\mathbf{d}$ is comprised between the lower and upper bound arrays, $\mathbf{D}_l$ and $\mathbf{D}_u$ respectively.

The following subsections detail the modelling strategies and tools used in this work, beginning with the energy system model developed using EnergyPLAN, and then reporting on the actual framework employed to solve the energy system co-design optimisation problem is described.

*2.1.1. Energy system model*

In the context of energy transition, energy system migration towards a maximised RES penetration needs to be supported by customised plans. With the aim to account for a reliable and accurate tool to support the development of such strategies, in literature, a plethora of energy systems modelling approaches and software have been developed [10]. As anticipated, the present study employs EnergyPLAN [58] as an energy system analysis tool.

EnergyPLAN is a deterministic input/output freeware developed by Aalborg University [9], it is widely employed in literature to perform hourly-based simulations of a designed energy system [9,59,60] and it is able to emulate with the same hourly resolution the complex interactions of the various energy sectors for entire energy systems [6,56,57,59,61]. The software receives as general inputs the electrical demands and the set of employed RES with their installed capacity and hourly-based generation distributions. Such distributions can be derived from empirically measured data or from modelling each RES power production considering their capacity to exploit the relative environmental resource.

In EnergyPLAN, it is also possible to easily design and integrate in the analysis other areas of interest of the investigated energy system, *i.e.* heating/cooling, industrial and other fuel consumption, desalination, transport and gas sectors, each one with its relative specifications and demand distributions. In addition to variable RES and traditional PP, the software is designed to also model different sources to supply the defined energy demands, including: waste to energy, liquid and gas alternative fuels (*e.g.* biofuel, biogas, electrofuel, hydrogen, hydrothermal liquification and pyrolysis). EnergyPLAN is also programmed to handle

various regulation strategies to deal with a critical excess of production or import/export necessities. After specifying additional energy system parameters in the software, such as costs and storage utilisation, the tool generates outputs including energy balances, annual production levels, fuel consumption, electricity import/export, and total costs, including cost and revenue from electricity exchanges. Moreover, the computational burden of simulating one year of operation for a given energy system in EnergyPLAN requires only a few seconds [10].

Therefore, given its characteristics, EnergyPLAN is an appropriate tool for modelling scenarios with high RES penetration interacting with other primary sectors of the energy system. Detailed description regarding the EnergyPLAN's mathematical model and algorithm can be found in the software documentation, available online at [62–64]. Together with the above mentioned characteristics, the fast computation capabilities of EnergyPLAN motivate the choice to employ this software in the present study with the aim to explore a wide range of potential energy system design in which integrate wave energy RES. On the other hand, despite the user friendly interface of the tool, it only allows a constrained number of subsequent simulations using its manual mode, ranging a limited number of design parameters for a defined energy system. To cope with the described limitations, the MATLAB Toolbox for EnergyPLAN [65] have been developed and successfully applied in previous studies [56,57,66], enabling the users to leverage EnergyPLAN's energy system analysis capabilities alongside MATLAB's computational advantages.

The present study employs the EnergyPLAN MATLAB tool in order to explore the search space of potential energy system designs that integrate ocean energy RES within a selected case study.

Accordingly, during the optimisation routine, the exploration of possible energy system configurations is performed in a MATLAB environment by researching over the set of possible energy systems' scenarios $\mathcal{E} \subset \mathbb{R}^{N_{RES}}$, where $N_{RES}$ represents the total number of distinct RES integrated into the energy system. Therefore, each energy system scenario is univocally defined by the energy system state vector $\mathbf{e} \in \mathcal{E}$, which elements are the RES installed capacity ($C_{RES_i}$, with $i \in \mathbb{N}_{N_{RES}}$). The installed capacity considered in the present study are the onshore and offshore wind energy ($C_{wind}$ and $C_{owt}$), solar photovoltaic ($C_{pv}$), and wave energy ($C_{wave}$).

In order to quantify the overall $CO_2$ emissions of the system, EnergyPLAN requires a detailed description of both energy supply and demand profiles with hourly resolution. This information are shaped by the energy system annual electrical demand ($D_e$), as well as the system's heating ($D_h$) and cooling ($D_c$) energy demands and their normalised hourly distributions ($\hat{\mathbf{D}}_e, \hat{\mathbf{D}}_h$ and $\hat{\mathbf{D}}_c$, respectively, with $\{\hat{\mathbf{D}}_e, \hat{\mathbf{D}}_h, \hat{\mathbf{D}}_c\} \subset \mathbb{R}^{N_y}$) with respect to the distribution's peak value. In addition, also the potentially exploitable production from the environmental resources, dependent from the investigated energy system's location, have to be imposed as constraints in the simulation. For these reasons, EnergyPLAN request to define the normalised hourly-based annual distribution for each involved RES, $\hat{\mathbf{P}}_{RES} \in \mathbb{R}^{N_y \times N_{RES}}$. Consistently with the previous mentioned installed capacity, in the present study we consider the normalised operative curves of both onshore and offshore wind ($\{\hat{\mathbf{P}}_{wind}, \hat{\mathbf{P}}_{owt}\} \subset \mathbb{R}^{N_y}$), solar ($\hat{\mathbf{P}}_{pv} \in \mathbb{R}^{N_y}$) and wave ($\hat{\mathbf{P}}_{wave} \in \mathbb{R}^{N_y}$) power

production. Also in this case the curves are normalised with respect to the distribution's peak value. In the present work, $\hat{\mathbf{P}}_{wind}$ has been obtained by normalising the wind hourly power production downloaded from the measured data given by the Red Eléctrica de España (REE) in [67]. Due to the lack of annual hourly-based production data, the normalised PV generation curve $\hat{\mathbf{P}}_{pv}$ is modeled directly based on solar irradiation as a general assumption, given that a more detailed representation within EnergyPLAN would have been excessively complex or unfeasible and beyond the purpose of the present study. The solar irradiation data have been obtained from Ref. [68]. Similarly, the operational curve of the offshore wind $\hat{\mathbf{P}}_{owt}$ is derived from the offshore mean wind speed resource, appropriately combined with the power curve of the wind turbine proposed in [69]. Regarding $\hat{\mathbf{P}}_{wave}$, the energy model receives the actual operational curve of the isolated WEC design as input directly from a previous WEC parametrisation stage; therefore it depends directly by each specific WEC design integrated in the energy system.

Spanning over each $h$-th hour among the $N_y$ hours of the year, the energy production for any $i$-th RES is evaluated as:

$$E^h_{RES_i} = C_{RES_i} \cdot \hat{P}^h_{RES_i}, \tag{6}$$

where $\hat{P}^h_{RES_i}$ is the normalised power produced by the $i$-th RES at the $h$-th hour, and therefore each RES's AEP as:

$$AEP_{RES_i} = \sum_{h=1}^{N_y} E^h_{RES_i}. \tag{7}$$

Subsequently, the RES' installed capacities have to be considered as an effective value. Therefore, for each $h$-th hour, the EnergyPLAN model evaluate $E^h_{RES_i} \forall i \in \mathbb{N}_{RES}$ and if their sum is lower than the $h$-th hourly value of the electricity demand ($\sum_{i=1}^{N_{RES}} E^h_{RES_i} < D^h_e$), it employs a conventional power plants (modeled by set an installed capacity $C_{PP}$ and plant efficiency $\eta_{PP}$) to fulfill the energy demand. In this way, the $CO_2$ emission can be calculated based on the PP power production, the transport fuel consumption $F_t$, and the natural gas demand ($N_{gas}$) requested by the energy system. Furthermore, each simulation includes the interaction of a Battery Energy Storage System (BESS) characterised by an installed energy capacity $C_{BESS}$, and maximum charge and discharge power capacities $S_{ch}$ and $S_{dis}$, respectively. The system operates with charge and discharge efficiencies denoted by $\eta_{ch}$ and $\eta_{dis}$, respectively.

In Fig. 3 is shown the block flowchart for the energy system simulation via EnergyPLAN is shown, while in Table 1, the list of involved parameters is reported.

### 2.1.2. Co-design optimisation framework

Now that all the essential components of the energy system model have been defined and declared, it is possible to describe its interaction with a generic WEC and, ultimately, to depict the co-design optimisation framework.

Generally, given a set $N_{WEC}$ WEC's design variables $\mathbf{w} \in \mathbb{R}^{N_{WEC}}$ in the WEC's design space $\mathcal{W} \subset \mathbb{R}$, the geometry, inertial properties and conversion system unit parametrisation of a single design are fully
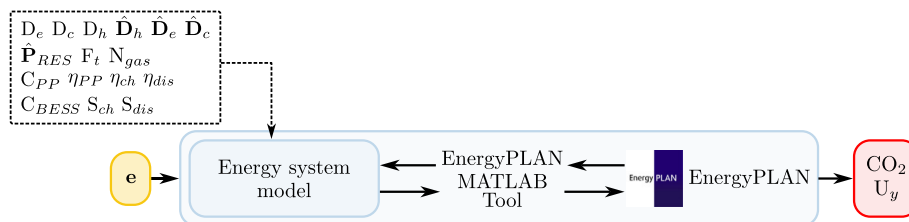


**Fig. 3.** Schematisation of the energy system model via EnergyPLAN. In the figure, **e** is the energy system state vector, while $\hat{\mathbf{P}}_{RES} = \{\hat{\mathbf{P}}_{wind}, \hat{\mathbf{P}}_{owt}, \hat{\mathbf{P}}_{wave}, \hat{\mathbf{P}}_{pv}\}$.

**Table 1**
List of the data involved in the EnergyPLAN simulation for the current study.

| Parameter | Unit | Description |
|---|---|---|
| $C_{wave}$ | (MW) | Wave energy installed capacity |
| $C_{pv}$ | (MW) | PV installed capacity |
| $C_{wind}$ | (MW) | Wind turbine installed capacity |
| $C_{owt}$ | (MW) | Offshore wind turbine installed capacity |
| $C_{PP}$ | (MW) | Conventional PP installed capacity |
| $C_{BESS}$ | (MWh) | BESS installed energy capacity |
| $\eta_{PP}$ | (/) | PP conversion efficiency |
| $N_{gas}$ | (GWh) | Natural gas demand |
| $F_t$ | (GWh) | Fuel consumption for transport sector |
| $D_e$ | (GWh) | Annual electricity demand |
| $D_c$ | (GWh) | Annual cooling demand |
| $D_h$ | (GWh) | Annual heating demand |
| $\hat{D}_e$ | (/) | Annual electricity demand normalised distribution |
| $\hat{D}_c$ | (/) | Annual cooling demand normalised distribution |
| $\hat{D}_h$ | (/) | Annual heating demand normalised distribution |
| $\hat{P}_{wind}$ | (/) | Annual wind energy production normalised distribution |
| $\hat{P}_{owt}$ | (/) | Annual offshore wind energy production normalised distribution |
| $\hat{P}_{pv}$ | (/) | Annual solar energy production normalised distribution |
| $\hat{P}_{wave}$ | (/) | Annual wave energy production normalised distribution |
| $S_{ch}$ | (kW) | Storage charge capacity |
| $S_{dis}$ | (kW) | Storage discharge capacity |
| $\eta_{ch}$ | (kW) | Storage charge efficiency |
| $\eta_{dis}$ | (kW) | Storage discharge efficiency |
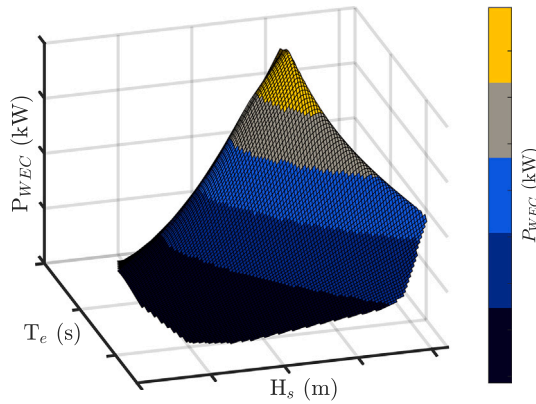


**Fig. 4.** Absorbed power map, interpolated over a $H_s - T_e$ grid for a set of representative waves for a generic WEC design.

identified and the analysis of the system can move towards the hydrodynamic and hydrostatic evaluation. Subsequently, the WEC dynamic responses to a set of waves representative of the site are computed, and the second-level PTO's control optimisation loop is performed. By interpolating the values of absorbed power for each of the representative sea states, it is possible to recreate a power surface over a $H_s$-$T_e$ grid and therefore evaluate the expected value for each of the non-zero occurrent $N_w$ waves. Fig. 4 shows the interpolated power surface over the $H_s$-$T_e$ grid for an exemplary WEC design. Now, to compute the absorbed power for the occurring sea states along the investigated year enables the estimation of the actual annual operational curve of the isolated WEC device. Then, the obtained hourly-distributed mean power absorbed $P_{WEC}$ is normalised ($\hat{P}_{wave}$) and, given the energy system state vector **e**, the annual behaviour of the energy system is simulated with the EnergyPLAN model and the energy system outputs, $CO_2$ emissions and $U_y$ are calculated.

In the present work, the multi-objective optimisation problem is solved in MATLAB environment by means of a Non-dominated Sorting Genetic Algorithm II (NSGA-II) [70] performed via "gamultiobj" function, setting 70 individuals for 150 generations. While the proposed co-design framework is agnostic to the specific optimisation algorithm

employed and can accommodate alternative methods, in this case NSGA-II was selected for its well-established ability to efficiently explore complex design spaces. Its robustness in handling non-convex and discontinuous solution landscapes makes it particularly suitable for the coupled WEC–energy system optimisation problem considered here. Moreover, the NSGA-II uses standard GA operators (selection, reproduction, crossover and mutation) but introduces a fixed percentage of elitism in the framework to enhance individual variability and facilitate a wide exploration of the design space, thereby minimising the risk of the optimiser to stuck in local minima. Instead, constraints have been addressed through the use of penalty functions. Both geometrically unfeasible and hydrostatically unstable solutions are managed using such penalty functions to guide convergence towards feasible solutions.

Currently, based on the data provided by the Canarian government concerning the installed battery capacity for the actually installed RES [71,72],[1] $C_{BESS}$ in La Gomera is 45 MWh. In the present work, such a value is fixed and kept constant during the overall optimisation in order to avoid BESS oversizing. Moreover, for the sake of simpicity the charge and discharge capacity ($S_{ch}$ and $S_{dis}$, respectively) have been set equal to 22.5 MW, corresponding to a charging rate of 0.5 (*i.e.* 2 hrs), with charging and discharging efficiency ($\eta_{ch}$ and $\eta_{dis}$) set equal to 0.9.

At last, in Fig. 5 the complete outline of the approach followed in the current article is shown. The presented structure is composed of 5 main steps, which are:

Step 1. The reference energy system under study is identified based on real-world scenario information for which official and verified data and reports are available. All key characteristics of the system are analysed, including the energy demands of various sectors, potential changes within each sector, and possible energy supply sources that could be exploited.

Step 2. Using the collected information, the reference energy system model is developed in EnergyPLAN. Then, the model is tuned and validated with respect to the actual benchmark data concerning $CO_2$ emissions and fuel consumption.

Step 3. Once the model has been validated, a set of possible alternatives for the energy system is identified together with the boundaries of the WEC's design space. In this way, the energy system co-design optimisation problem given in Section 2 can be formulated.

Step 4. The optimisation routine explores the design space $D$ until the maximum number of generations is exceeded. For each individual, the relative WEC's design operational curve is obtained and used as input in the energy system annual simulation via EnergyPLAN and the output ($CO_2$ and $U_y$) is collected.

Step 5. When the convergence criteria (*i.e.* the maximum number of generations) are reached, the GA stops and the results are collected and discussed.

## 3. Case of study: La Gomera

In the Canary archipelago, the minor island of La Gomera has been chosen as a case study to test the presented optimisation framework. Located near the African coast and about 1350 km far from Europe, the Canary archipelago is a Spanish autonomous community and the outermost region of the European Union. The geographical location of the La Gomera island is illustrated in Fig. 6.

The Instituto Canario de Estadistica (ISTAC) reports that in 2023, the La Gomera's inhabitants were around 22,162 people [73], corresponding

---

[1] According to the referenced documents, two battery packs of 4.5 MWh each are installed for three out of the five wind turbines that make up the La Gomera wind farm. In this study, it is assumed that the same BESS capacity per wind turbine is installed uniformly across all five turbines currently operating in La Gomera.
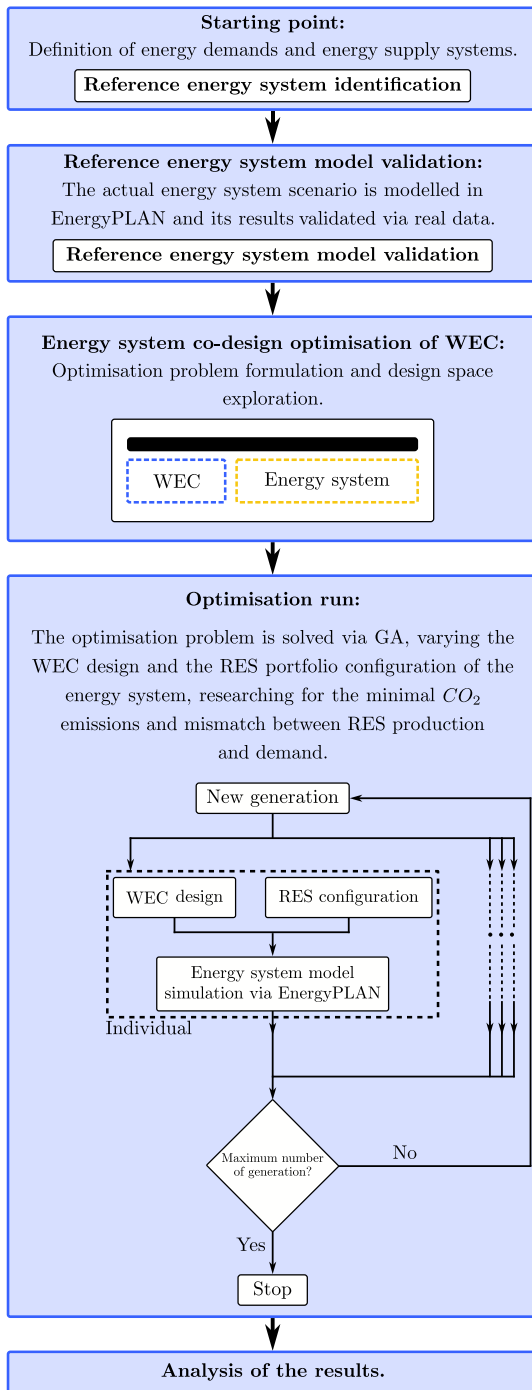
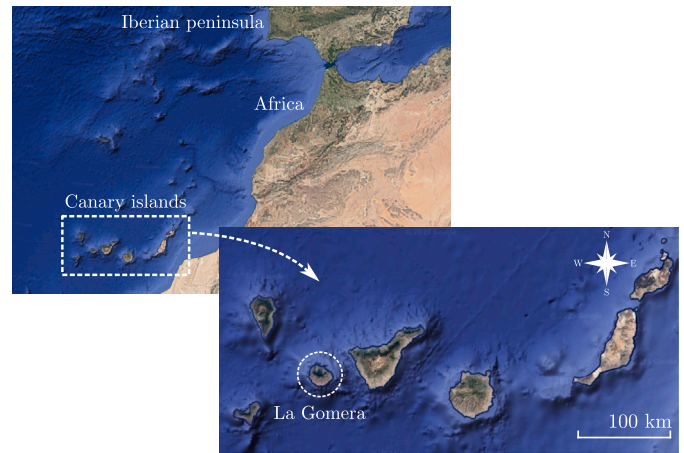Fig. 5. Outline of the proposed approach.



**Fig. 6.** Geographical location of La Gomera island.

Therefore, the first twelve months of wind turbines operations have been chosen as reference time for the simulations performed, *i.e.* between the fist day of April 2023 to the last day of March 2024. Such a low level of RES penetration allows us to consider La Gomera as a good benchmark study with the aim of providing data and proposing solutions for its transition towards a more sustainable energy system.

Delving into the La Gomera energy system description, the analysis of the transport sector focuses solely on road transport, as it is the only mode exclusively related to the island. In contrast, aviation and maritime transport, despite their fuel consumption, are considered international concerns and are therefore excluded. Sources indicate that La Gomera's road transport sector is almost entirely dependent on oil, with an annual consumption of 5.1 kt of gasoline and 6.8 kt of diesel, while electricity contributes only 0.13 GWh/y [74]. Regarding natural gas consumption on the island, the 2022 annual report of the Canarian government reports a usage of 10.42 GWh/y. Moreover, since the reference documents do not specify the exact applications of natural gas, some assumptions have been made. Given that La Gomera lacks a district heating system due to its typical warm climate, it was inferred that natural gas in private households is used exclusively for cooking and not for heating. In contrast, within the broader category of hotels and services, it is assumed to be partially used for heating as well. Based on these assumptions and data from Ref. [73,75], the distribution of gas consumption across different sectors was estimated. Due to lack of a government official report for 2023, the presented data concerning natural gas and transport consumption refer to the government report of 2022 and have also been assumed for the timeframe under analysis. For what concern the water treatment energy consumption, La Gomera lacked a desalination plant in 2022, but a 3000 m$^3$/day facility was installed in March 2024, with its energy use included in general electricity demand. Wastewater treatment processes 1.03 hm$^3$ annually, requiring an estimated 0.9 GWh/y based on government reports and studies on other islands [57,76]. To estimate the energy distribution for heating, cooling, domestic hot water, and kitchen use, statistical data from ISTAC [73] were cross-referenced with a government report in collaboration with the University of La Laguna [75].

Two main consumer categories were identified: households and hotels/services. Household electricity consumption was estimated at 27.3 GWh, with cooling accounting for 10.9 % and domestic hot water for 13.3 %. Hotels and services consumed 29.71 GWh of electricity and 5.41 GWh of natural gas, with 30.8 % used for cooling and 22 % for heating, covering domestic hot water, pool maintenance, and space heating. Heating demand was assumed to be periodically distributed for each day of the year, while cooling demand was distributed based on hourly temperature data, activating when temperatures exceeded 22 °C, with 65 %
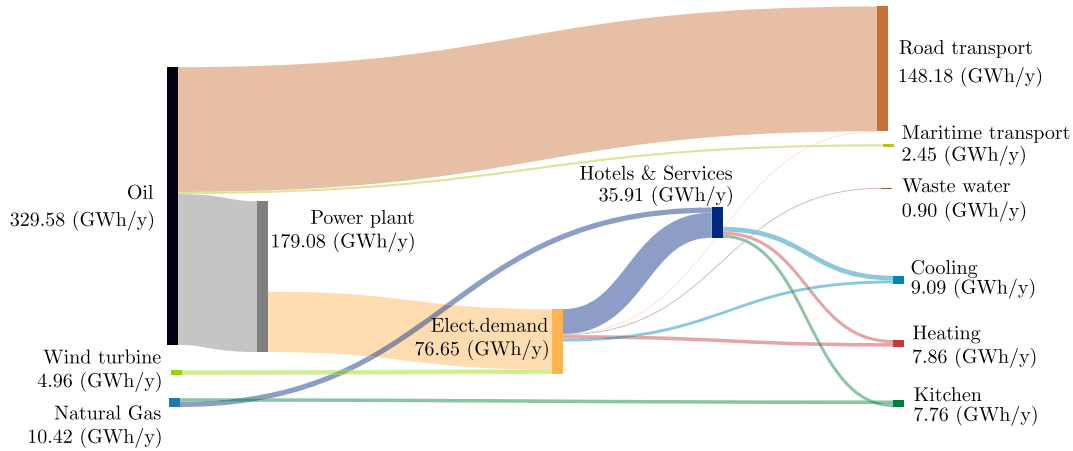
to an electrical demand of 71.69 GWh/y according to the open data given by the local Transmission System Operator (TSO), i.e. REE [67].

Despite the considerable RES potential, according to the national annual reports [74], the energy supply of the La Gomera energy system deeply relies on the 21 MW of installed capacity at the El Palmar thermal power plant. However, by the end of March 2023, the installation of a 12 MW wind turbine power plant had been completed, but only 2.23 MW are now operative. Moreover, in [69] it is pointed out that La Gomera presents the largest suitable area for offshore RES installation with respect to the other islands of the archipelago. These carachteristics of La Gomera make it a valuable case study for the purpose of the present study.

**Fig. 7.** Sankey diagram of the La Gomera energy system. The diagram is based on the methodology and input data described in Section 3.
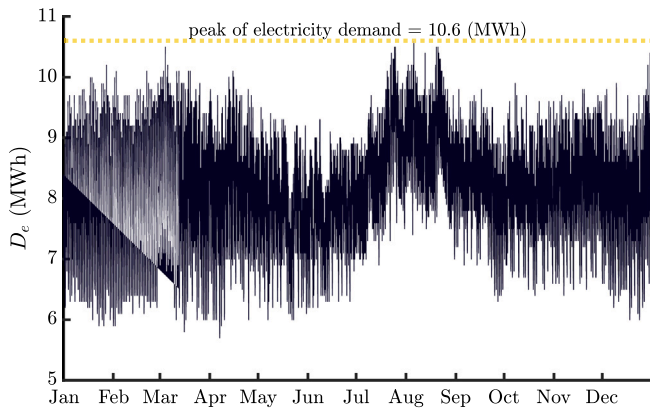


**Fig. 8.** Electricity demand ($D_e$) of La Gomera in 2022. Data from Ref. [67].

**Table 2**

$CO_2$ emissions (transport and electricity supplied by PP) and $F$ consumption validation for 2022. Reference value data are achieved from Ref. [74].

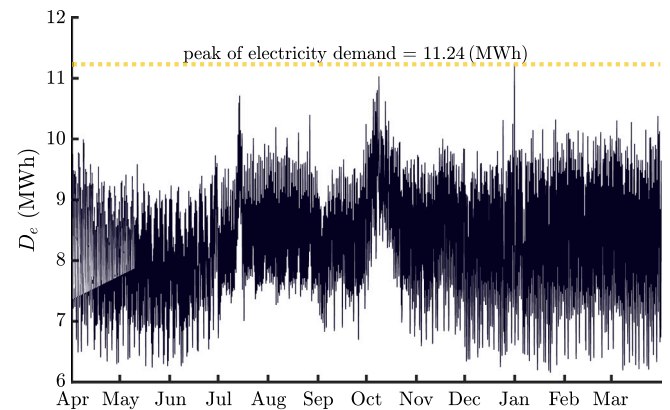| Parameter | EnergyPLAN model | Reference value | Error |
|---|---|---|---|
| $CO_2$ | 92.9 kt | 98.3 kt | 5.5 % |
| $F$ | 186.5 GWh/y | 186.2 GWh/y | 0.2 % |



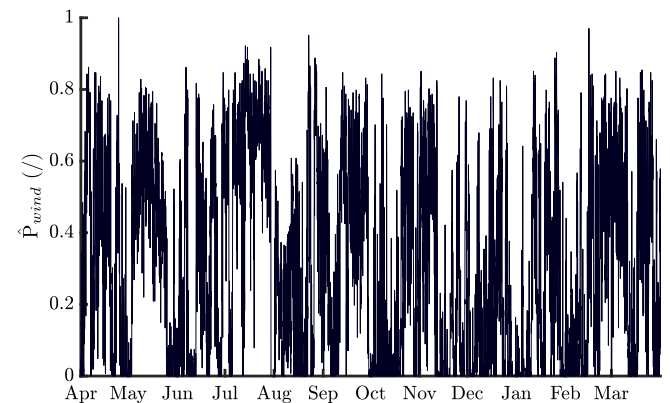**Fig. 9.** Electricity demand ($D_e$) of La Gomera between april 2023 and march 2024. Data from Ref. [67].



**Fig. 10.** Normalised wind energy production distribution ($\hat{P}_{wind}$) between April 2023 and March 2024. data from Ref. [67].

of demand evenly allocated to account for continuous air conditioning use in service areas. The Sankey diagram of the La Gomera energy system is illustrated in Fig. 7.

### 3.1. La Gomera energy system identification and reference model validation

Exploiting the hourly data shared by the REE [67] and the information given in the national annual reports [74], an EnergyPLAN reference model has been developed and validated.

At first, a 2022 energy system model of La Gomera has been developed with respect to the El Palmar PP fuel consumption ($F$) and the overall energy system $CO_2$ emissions, in order to test and validate the outcomes for what concern the natural gas and transport consumption and emissions that are assumed also for the time period of interest. For the 2022 EnergyPLAN model, the reference value have been set referring to [74] considering a electric demand of 69 GWh/y distributed as described in Fig. 8, the same water treatment plant, while households and hotels consumption are derived again from Ref. [73,75] and are equal to 37.4 GWh/y and 34.1 GWh/y with the same proportion and distributions described above. The results present a complete validation of the model and are reported in Table 2.

Now, the EnergyPLAN system model can be validated by referring to the fuel emissions and $CO_2$ emissions (referring to the kt$_{eq}$ given by the local TSO in [67]) only for the hourly simulated PP production, considering the 2023–2024 electricity demand and the wind power supply distribution reported in Figs. 9 and 10, respectively. The results demonstrate a good reliability of the model, with levels of mismatch lower than

**Table 3**
$CO_2$ emissions (transport and electricity supplied by PP) and $F$ consumption validation for 2023–2024. Reference value data are achieved from Ref. [67].

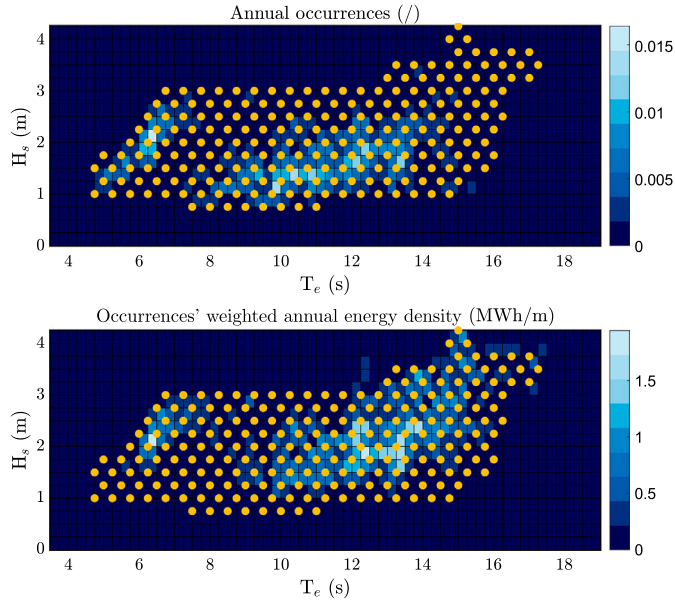| Parameter | EnergyPLAN model | Reference value | Error (%) |
|---|---|---|---|
| $CO_2$ | 888.6 $kt_{eq}$ | 882.3 $kt_{eq}$ | 0.71 % |
| $F$ | 177.4 GWh/y | 173.1 GWh/y | 2.5 % |



**Fig. 11.** Map of the annual occurrences and the occurrences' weighted annual energy density map per meter of wavefront of La Gomera. Yellow dots identify the set of representative waves employed in the PTO control optimisation. data from Ref. [77].

the 3 % of the reference values. The validation outcomes are reported in Table 3.

### 3.2. La Gomera wave energy resource

Focusing on La Gomera's wave energy resource, the occurrences and the occurrences' weighted annual energy density map per meter of wavefront are shown in Fig. 11. The two heatmaps reveal two area of major occurrences: the first around 6 s of $T_e$ with roughly 2 m of $H_s$, while the second area lies around 10 s of $T_e$. To balance map coverage and computational time, a set of representative waves is identified and plotted as yellow dots on both the energetic and occurrence maps. The selected set of waves will then be employed in the optimisation phase of the PTO

control parameters as discussed above. The occurrences' weighted site's annual power density for meter of wavefront is 17.0 kW/m.

### 3.3. WEC numerical model

#### 3.3.1. Working principle, governing equation and mathematical model

As anticipated, the energy-system aware optimisation framework presented in this study aims to investigate the performance of possible design solutions for the PeWEC, in order to explore the optimal designs able to provide benefits of wave energy to an off-grid island energy system. The PeWEC, developed at the Marine Offshore Energy Lab of Politecnico di Torino in collaboration with ENEA, presents a well-established research literature [78–88], supported by extensive experiments and numerical validations [89,90].

The PeWEC is an inertial-based floating device [91] in which the floater pitch motion, induced by incoming waves, drives the spin of an enclosed pendulum around its rotational axis ($\varepsilon$). The electricity conversion is effected by means of a PTO unit, which is connected to the pendulum by a gearbox. The fully enclosed design of the system enhances the WEC's reliability in the harsh marine environment, while four mooring lines are designed to guarantee simultaneously both the pitching motion and the device's station-keeping in both operational and severe sea state conditions. Figs. 12 and 13 illustrate the PeWEC design with its internal components schematisation and the system working principle, respectively.

A state-of-the-art linear frequency domain approach has been employed, enabling to performance of the design optimisation routine with a good trade-off between accuracy and computational burden. The numerical model, experimentally validated [89,90], integrates the linear frequency domain in order to simulate the WEC's dynamics [81,92] while the device's floater hydrodynamics coefficients are evaluated under linear potential-flow theory assumptions [30,93]. Moreover, it is reasonable to investigate mono-directional waves and therefore to represent the system state of motion $\mathbf{u} \in \mathbb{R}^4$ as:

$$\mathbf{u} = \left[ x, z, \delta, \varepsilon \right]^T, \tag{8}$$

where $x$ (surge) is the translation along the $x$-axis, $z$ (heave) is the translation along the $z$-axis, while the rotation with respect to $y$-axis and pendulum axis are $\delta$ and $\varepsilon$, respectively. The main mathematical equation governing the WEC dynamics is formulated as [81]:

$$[\mathbf{M} + \mathbf{A}(\omega)] \ddot{\mathbf{u}} + \mathbf{B}(\omega) \dot{\mathbf{u}} + \left[ \mathbf{K}_h + \mathbf{K}_p \right] \mathbf{u} = a_\omega(\omega) \mathbf{F}_\omega(\omega) + \mathbf{T}_{PTO}, \tag{9}$$

that in the frequency domain formulation becomes [82]:

$$-\omega^2 [\mathbf{M} + \mathbf{A}(\omega)] \mathbf{u}(\omega) + j\omega \mathbf{B}(\omega) \mathbf{u}(\omega) + \left[ \mathbf{K}_h + \mathbf{K}_p \right] \mathbf{u}(\omega)$$
$$= a_\omega(\omega) \mathbf{F}_\omega(\omega) + \mathbf{T}_{PTO}(\omega), \tag{10}$$
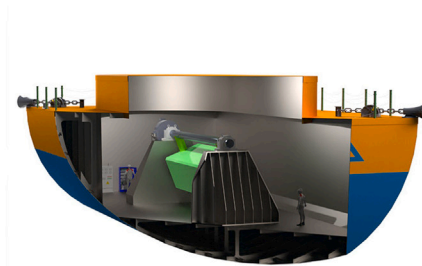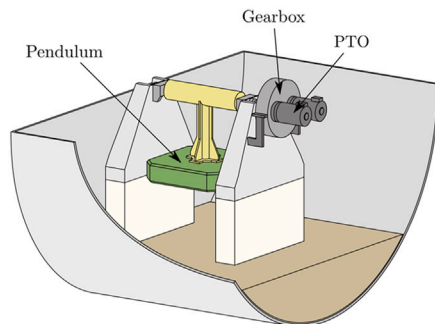


**Fig. 12.** On the right, the full-size PeWEC 3D-render and on the left, a CAD schematisation of the internal WEC components.
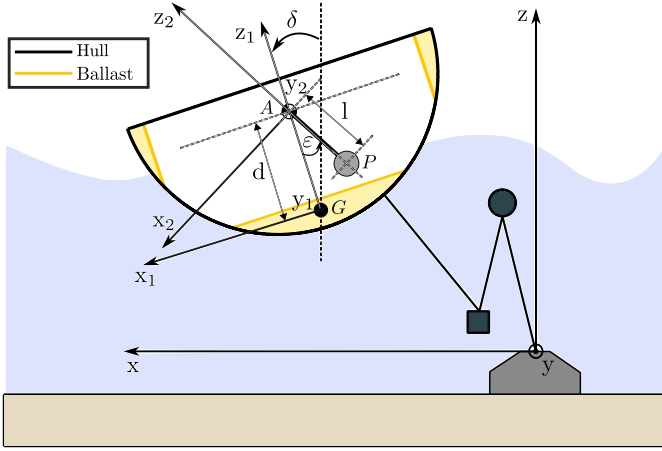
**Fig. 13.** PeWEC device's working principle and its relative coordinates reference systems. Adapted from Ref. [78].

where: $\{\mathbf{M}, \mathbf{K}_h, \mathbf{K}_p\} \subset \mathbb{R}^{4 \times 4}$ are the mass matrix, the hydrostatic stiffness matrix and the pendulum restoring force, respectively, while $a_\omega(\omega) \in \mathbb{R}^4$ is the wave amplitude and $\omega$ is the frequency.

In this study, a boundary element method (BEM) solver, such as NEMOH [94], is exploited to determine the hydrodynamic parameters within the frequency domain. Specifically, the BEM computes the added mass, radiation damping and waves' excitation coefficients, expressed as $\{\mathbf{A}(\omega), \mathbf{B}(\omega)\} \subset \mathbb{R}^{4 \times 4}$ and $\mathbf{F}_\omega(\omega) \in \mathbb{C}^4$, over a selected range of representative frequencies. In the equation, $\mathbf{u}(\omega)$ indicates the Fourier transform of the WEC's state of motion [30]. The pendulum-unit and hull coupling can be depicted by the inertial and restoring force contributions in [81,88]:

$$\mathbf{M} = \begin{bmatrix} (m_h + m_p) & 0 & m_p(d - l) & -m_p l \\ 0 & (m_h + m_p) & 0 & 0 \\ m_p(d - l) & 0 & I_h + I_p + m_p(d - l)^2 & I_p + m_p l^2 - m_p dl \\ -m_p l & 0 & I_p + m_p l^2 - m_p dl & I_p + m_p l^2 \end{bmatrix},$$ 

(11)

$$\mathbf{K}_p = \begin{bmatrix} 0 & 0 & 0 & 0 \\ 0 & 0 & 0 & 0 \\ 0 & 0 & -gm_p(d - l) & gm_p l \\ 0 & 0 & gm_p l & gm_p l \end{bmatrix}.$$ 

(12)

In the matrices, the hull and pendulum masses are represented by $m_h$ and $m_p$, respectively, while g denotes the gravitational acceleration. $I_h$ and $I_p$ refer to the hull and pendulum inertia. Instead, d and l are corresponding to $\overline{GA}$ and $\overline{PA}$ in Fig. 13, *i.e.* the distances between the WEC's centre of gravity and the pendulum's oscillation axis, and the length of the pendulum arm.

Moreover, $\mathbf{T}_{PTO}(\omega) \in \mathbb{R}^4$ represents the PTO torque action on the pendulum's rotational degree of freedom. In order to increase the energy harvested by the system, in the WECs area of research it is a widely adopted practice to develop tailored control strategies to maximise the absorbed energy [95–97]. Readers can found some previous studies regarding the development of control strategies for the PeWEC in [84–88]. However, in the present work, a first-order transfer function control law is implemented, defined as:

$$T_{ctrl}(\omega) = \frac{j\omega \alpha_{PTO}}{j\omega + \beta_{PTO}},$$ 

(13)

where $\alpha_{PTO} \in \mathbb{R}^+$ and $\beta_{PTO} \in \mathbb{R}^+$ are the optimised control parameters, belonging to the positive set of real numbers ($\mathbb{R}^+$). Such formulation

ensures the system stability, while achieving optimal energy extraction, thanks to its passivity property [98]. The control action contributes to the PTO control as follows:

$$T_{PTO}(\omega) = \frac{T_{ctrl}(\omega)}{\tau_{gear}},$$ 

(14)

$$\mathbf{T}_{PTO}(\omega) = \begin{bmatrix} 0, 0, 0, T_{PTO}(\omega) \end{bmatrix}^T,$$ 

(15)

in which $\tau_{gear}$ is the pendulum-PTO's unit gearbox ratio, $T_{PTO}(\omega)$ is the torque generated by the PTO, and $T_{ctrl}(\omega)$ is the control torque acting on the $\varepsilon$-axis. Therefore, the absorbed power $P_{WEC}$ of the system is generally expressed as:

$$P_{WEC}(\omega) = \int_0^\infty \text{Re}\left\{ T_{ctrl} S_{\dot{\varepsilon}\dot{\varepsilon}}(\omega) \right\} d\omega,$$ 

(16)

with $T_{ctrl}(\omega)$ as described in Eq. (13) and $S_{\dot{\varepsilon}\dot{\varepsilon}}(\omega)$ the power spectal density [99] of the $\varepsilon$-axis rotational velocity:

$$\dot{\varepsilon} = j\omega \varepsilon(\omega).$$ 

(17)

In the framework, a control optimisation process seeks to maximise the WEC's extracted power by adjusting the two control parameters for a set of $N_c$ simulated representative waves, which are modelled according to a joint north sea wave project (JONSWAP) spectrum [100,101]. During the optimisation, an a posteriori validation is performed to ensure consistency with the operational constraints imposed by the mechatronic system. Any parameter pairs exceeding these limits are discarded. In particular, the generator's rotational speed must remain below its rated threshold, and the PTO torque must not exceed its nominal specification. Subsequently, after achieving a set of optimal control parameters $\{\alpha_{PTO}^{opt}, \beta_{PTO}^{opt}\} \subset \mathbb{R}^{2 \times N_c}$, the AEP for the PeWEC is evaluated as:

$$AEP_{WEC} = \frac{3600 \cdot 24 \cdot 365}{100} \sum_{i=1}^{N_w} Occ_\%^i P_{WEC}^i(\omega),$$ 

(18)

with $i$ as the index counting the $N_w$ simulated sea states with non-zero occurrences percentage ($Occ_\%^i$), and $P_{WEC}^i(\omega)$ is the mean absorbed power of the i-th occurrent sea state if the optimal control parameters set $(\alpha_{PTO}^{i,opt}, \beta_{PTO}^{i,opt})$ is applied.

Consistent with the methodology employed in the previous studies [81,88], further assumptions have been made to ensure the linearity of the numerical model, thereby enhancing computational efficiency. In particular, drift and second-order forces, mooring effects, and viscous damping are neglected, as well as PTO power losses. Despite these simplifications, the proposed model is suitable for a preliminary design exploration phase, consistent with the general techno-economic objectives of this research. Moreover, the quite low computational burden of the model allows us to explore a wide area of the design space by means of a high number of simulations.

### 3.3.2. WEC design parametrization

In the present work a parameterised approach (already applied in [81]) is employed to implement the PeWEC mathematical model and evaluate its performance for a given system's design along in each hour of the simulated year.

Similarly to previous studies on PeWEC design optimisation, the hull shape (*i.e.* a key driver of device performance optimisation [50] due to its influence on the wave-hull hydrodynamic interaction [93]) is parameterised according to the schematisation shown in Fig. 14. The profile section of the device in the x-z plane exhibits a curved geometry, consisting of a bottom circumference that is tangential to two additional circumferences positioned at the bow and stern. The floater is symmetric with respect to both the y-z and x-z planes, and the full volume is obtained by extruding the hull's profile along the y-axis.

The mass and inertia of the WEC, critical to both cost and performance, are parameterised following established methodologies derived from previous experiences [81]. The equivalent structural thickness is derived based on the floater's surface area and structural mass ($m_h$). The hull is constructed from naval-grade steel ($\rho_h = 7800 \text{ kg/m}^3$), while sand ($\rho_b = 1400 \text{ kg/m}^3$) is selected as ballast due to its favourable cost-to-weight ratio.

Concerning the pendulum unit, its mass ($m_u$) is defined by adding a 40 % mass housing coefficient to the pendulum mass ($m_p$) to account for the support structure, PTO, and gearbox. The unit consists of a steel parallelepiped mass ($\rho_p = \rho_h$) with dimensions $\zeta$ x $\phi$ x $l_p$, positioned at a distance $l$ from the fulcrum. Setting $m_p$, $\zeta$, and $\phi$ as design variables, the pendulum's mass dimension $l_p$ is derived geometrically, while the fulcrum height is correlated with the unit position parameter ($\lambda_0$), also ensuring the complete pendulum rotation. The conversion stage employs a PTO system with a permanent magnet synchronous motor and a high-torque, low-speed gearbox. In the PeWEC parametrisation, the PTO is defined by a specific ID, selecting one of 37 options characterised by nominal speed, gearbox ratio, and torque.

In conclusion, each PeWEC device is fully defined by a set of 13 design variables:

- the total WEC's size along the x-axis, namely the hull length $L$;
- the total WEC's size along the y-axis, namely the hull width $W$;
- the bow-circumference shape parameter, namely $h = x_A / \frac{L}{2}$;
- the height-draft ratio parameter, namely $k = x_A / \frac{H}{Dr}$;
- the hull-draft ($Dr$) parameter, namely $\alpha$, which establishes a maximum pitch angle during operation to avoid excessive green water from spilling over the device deck;
- the ballast filling ratio (BFR), which quantifies the distribution of ballast across the fore, aft, and keel tanks. The BFR, ranging from 0 to 1, compares the ballast in the stern and bow tanks to the total ballast of the WEC. Fig. 14 illustrates how increasing the BFR influences ballast inertia distribution;
- the pendulum mass, namely $m_p$;
- the pendulum arm length, namely $l$;
- the pendulum mass width, namely $\phi$;
- the pendulum mass height, namely $\zeta$;
- the number of $N_u$ pendulum units;
- the unit position $\lambda_0$;
- the PTO unit ID.

Moreover, Table 4 reports the lower and upper boundaries among which each element of **d** is comprised between.

**Table 4**
GA's free variables for the definition of a singular individual.

| Design parameter (**d**) | Unit | Lower bound ($\mathbf{D_l}$) | Upper bound ($\mathbf{D_u}$) |
|---|---|---|---|
| Hull length - $L$ | (m) | 10 | 30 |
| Hull width - $W$ | (m) | 5 | 25 |
| Hull shape ratio - $h$ | (/) | 0.4 | 1 |
| Hull heigth ratio - $k$ | (/) | 0.4 | 1 |
| Hull draft parameter - $\alpha$ | (/) | 15 | 25 |
| Ballast filling ratio - BFR | (/) | 0.1 | 1 |
| Pendulum mass - $m_p$ | (kg) | 5000 | 30,000 |
| Pendulum arm length - $l$ | (m) | 0.5 | 5 |
| Pendulum mass width - $\phi$ | (m) | 0.5 | 2.5 |
| Pendulum mass heigth - $\zeta$ | (m) | 0.45 | 2.5 |
| Number of pendulum units - $N_u$ | (/) | 1 | 4 |
| Unit position - $\lambda_0$ | (/) | 1 | 1 |
| PTO ID | (/) | 1 | 37 |
| PV installed capacity - $C_{pv}$ | (MW) | 0 | 150 |
| Wind turbine installed capacity - $C_{wind}$ | (MW) | 12 | 150 |
| Wave energy installed capacity - $C_{wave}$ | (MW) | 0 | 150 |
| Offshore wind turbine installed capacity - $C_{owt}$ | (MW) | 0 | 150 |

### 3.3.3. WEC costs

Regarding the parameterisation of WEC costs, they are formulated referring to the bottom-up approach described in [83]. In assessing the WEC's cost major drivers, multiple factors are considered. Hull costs are primarily dictated by the structure's mass and material expenses, which also include accessory costs. The PTO system's cost depends on its type and size, while mechanical components such as the pendulum, basement, shaft, and joints are added to the total cost, including assembly. Additionally, electronic component costs are determined by the power rating of the WEC. Mooring and installation expenses are considered as well, both assumed to account for 15 % of the total cost.

Given the early stage of their technological industrialisation, WECs are not yet cost-competitive compared to more mature RES technologies. However, recognising the high potential of wave energy, ambitious global targets have been set, supported by proactive strategies aimed at reducing energy costs. Studies suggest that cost reduction can be achieved through technological advancements and the development of an innovative ecosystem that integrates policy support, financial incentives, continuous innovation, and niche market expansion [102–106]. Based on the referred techno-economic projections, this study assumes a 50 % reduction in PeWEC's current $CapEx$, driven by increased installed capacity and improved learning rates in the industrialisation process [104,107,108]. Additionally, a 100 % increase in absorbed power is considered, reflecting advancements in technological performance,
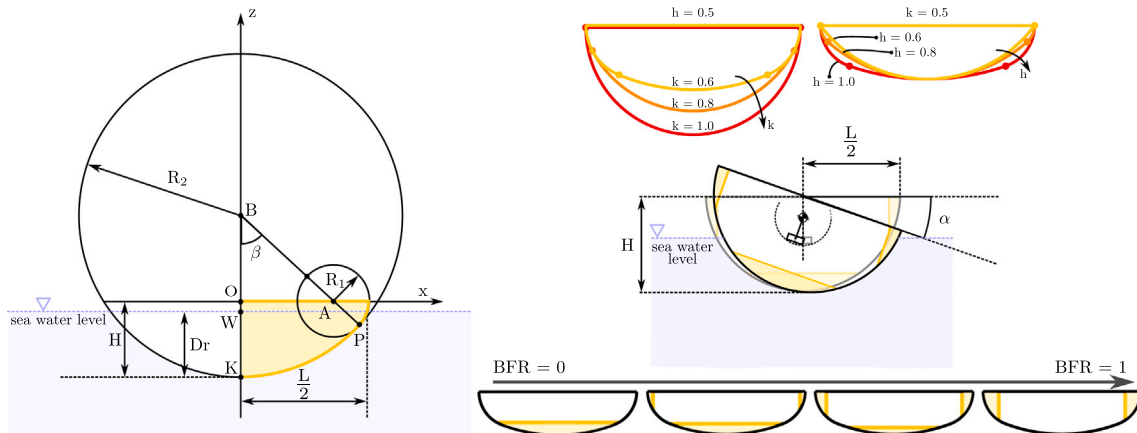


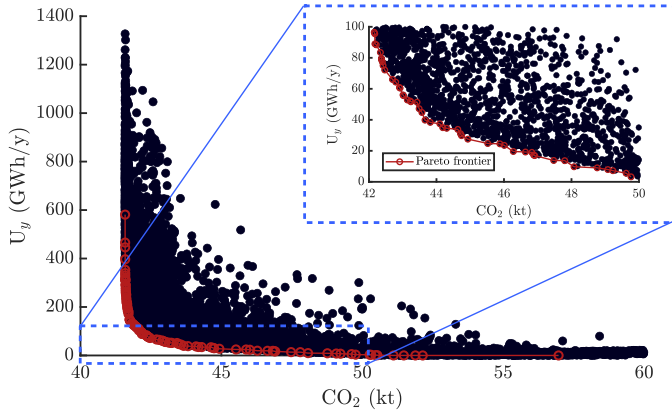**Fig. 14.** Schematisation of geometric PeWEC design variables.

**Fig. 15.** Energy system co-design optimisation outcomes. In red, the Pareto frontier. In the window, the area of major interest for the analysis.



**Fig. 16.** Focus on the $AEP_{WEC}$ map of the optimisation outcomes' region of interest.



**Fig. 17.** Focus on the WEC's $CapEx$ map of the optimisation outcomes' region of interest.



**Fig. 18.** Focus on the normalised CôE map of the optimisation outcomes' region of intrest.

particularly through the implementation of optimised control strategies [87,109].

The lack of long-term operational data for offshore WEC plants limits the reliability of $OpEx$ estimates [110]. $OpEx$ depends on device characteristics, such as design and size, as well as external factors like resource variability, extreme events, maintenance strategies, and industry learning [111–115]. Typically, $OpEx$ is estimated as a percentage of total investment, with reported values ranging from 1.4 % to 7 % [110,113–115]. In this study, $OpEx$ is assumed as a fixed 5 % of the total cost.

## 4. Results

The collected outcomes from the optimisation stage are depicted in Fig. 15. The optimisation problem solutions reveal a marked trade-off between the $CO_2$ emissions and the unexploited energy due to a mismatch between RES production and electric demand. Looking to the overall results, the set of solutions forming the Pareto frontier exhibits $CO_2$ emissions ranging approximately from 41.5 kt to 60 kt, corresponding to a potential reduction from the initial 88.8 kt of roughly 53 % and 32 %. As shown in Fig. 15, the Pareto curve becomes asymptotic to the horizontal and vertical axes near its endpoints. This behaviour suggests that, for low emission levels, even minor reductions in $CO_2$ come at the cost of large increases in $U_y$. Conversely, for low $U_y$ values, small improvements require substantial increases in emissions. To better focus the analysis, the most dynamic portion of the Pareto front (*i.e.* the so-called elbow) has been emphasised. This area, characterised by higher solution density and gradient, corresponds to approximately 42 to 50 kt of $CO_2$ and 0 to 100 GWh/y of $U_y$.

Figs. 16 and 17 employ a color-coded representation to depict the spatial variation in $AEP_{WEC}$ and $CapEx$ for WECs located within the identified region of interest. The results reveal that the most productive WECs do not necessarily lie on the Pareto front. This finding underscores a critical consideration in energy systems integration: the value of a renewable energy converter lies not merely in its maximal generation capacity (*i.e.* maximum productivity is not the sole priority), but in its ability to contribute effectively during periods of demand. In this context, productive synergy with other RES becomes a fundamental design criterion. Concerning $CapEx$, the Pareto-optimal systems tend to cluster around a cost of approximately 6 mln€, representing a balanced trade-off rather than the most expensive or cheapest configurations observed.

The outcomes are further analysed with respect to the cost of energy (CoE), calculated as the ratio between $CapEx$ over the total AEP generated over 25 years of plant operation. As shown in Fig. 18, the
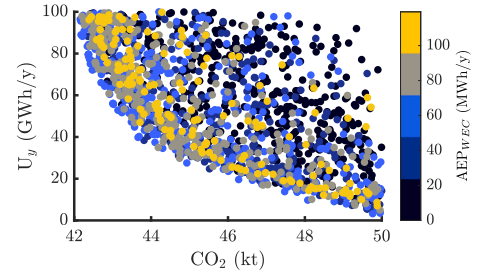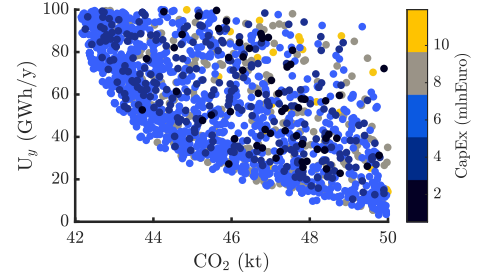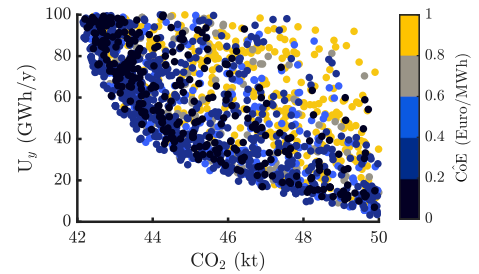
resulting distribution reinforces previously established trends: the optimiser selects a Pareto front of design solutions for which the CoE is approximately 40 % of the maximum observed value across all simulations.

Fig. 19 presents the installed capacities of RES and the corresponding annual peak of hourly PP production for scenarios on the Pareto front. In the simulation framework, PP units are dispatched only when RES generation fails to meet demand. Thus, the peak PP production reflects the required PP capacity in each scenario. Results indicate that this capacity ranges between 9.5 and 11 MW, implying a substantial reduction of approximately 50 % from the starting requirement of 21 MW.

The share of RES in the energy mix across the Pareto-optimal scenarios ranges from 70 % to 90 %, representing a substantial improvement from the initial baseline of 8.5 %. This transition illustrates the potentiality of configuring a high-RES energy system on the La Gomera island, while significantly decreasing the system's dependency on conventional thermal power generation.

The presented possible configurations, however, do not represent the theoretical upper limit of RES integration. Further improvements in system performance and resilience could be achieved through a series of complementary strategies. These include the optimal sizing and control of BESS, the development of alternative interconnection schemes with the neighbouring island of Tenerife [116], and the progressive
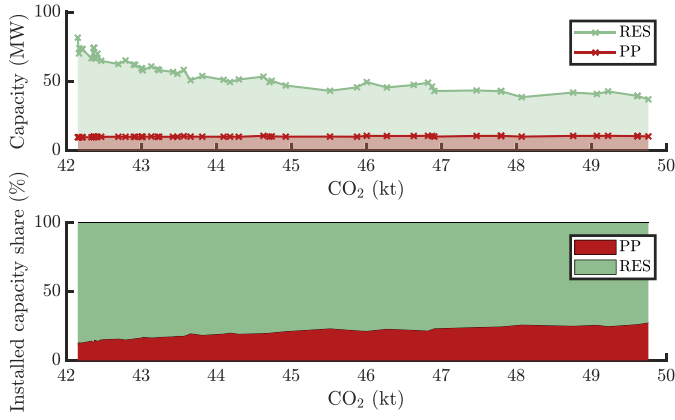
**Fig. 19.** RES and PP installed capacity trends of Pareto set scenarios concerning the increase of the $CO_2$ emissions.
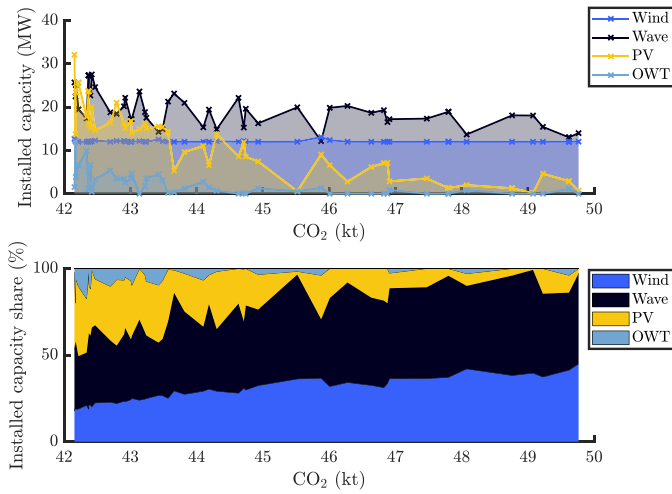


**Fig. 20.** Installed capacity trends of Pareto set scenarios for each employed RES, with respect to the increase of the $CO_2$ emissions.

electrification of end-use sectors, particularly transportation. While the aforementioned elements are beyond the current scope, the methodology introduced in this work (a generalisable co-design framework for the integration of WECs into broader energy systems) offers a robust foundation for their inclusion in future investigations. The adaptability of this approach makes it well-suited to support both energy system planning

studies and RES technology design. It is worth acknowledging that the proposed approach and resulting configurations must ultimately be supported by detailed techno-economic and regulatory feasibility studies. However, the method and results presented in this work offer a strong indication of plausible pathways for future energy system planning and RES deployment.

Focusing on RES, Fig. 20 illustrates the distribution of installed capacities across different RES technologies. The analysis reveals that the optimisation process tends to prioritise configurations with a relatively high installed capacity of wave energy. In scenarios characterised by higher $CO_2$ emissions but reduced annual unexploited renewable production ($U_y$), the installed capacities of wave and wind energy tend to converge to similar values. This preference can be attributed to the higher operational continuity of wave energy compared to PV, whose contribution is notably reduced in this segment of the Pareto front. Conversely, the results indicate that further reductions in $CO_2$ emissions require a more diversified RES portfolio. In such low-emission scenarios, both PV and OWT capacities increase to support the system's decarbonisation goals. However, a closer inspection of the RES share reveals that OWT remains the least installed RES technology across the full $CO_2$ emission range. While PV and wave energy capacities share are relatively similar under low-emission conditions, PV capacity declines as $U_y$ levels decrease. Meanwhile, wind energy installations remain relatively stable, with installed capacity consistently around 12 MW across all scenarios.

Fig. 21 illustrates the optimisation outcomes for key WEC design parameters. Among them, hull length ($L$) and pitch resonance period ($T_{res}^\delta$) exhibit the most consistent trends across the Pareto front, excluding isolated outliers. The results converge around a hull length of 30 m and a resonance period of approximately 9 s, aligned with the most prevalent wave periods observed in the site, albeit not those with the highest energy content. Conversely, the analysis reveals no definitive trends for the remaining parameters, including hull width ($W$), height ($H$), pendulum mass ($m_p$), and displaced mass.

In Fig. 22, the wave power distribution envelopes are presented for the complete set of WEC design configurations evaluated during the optimisation process (blue), in contrast to those corresponding to the Pareto-optimal designs (black). The full WEC design space exhibits a broad range of possible operational power curves, reflecting the diversity of explored design parameters. However, the distributions associated with Pareto-optimal solutions are notably narrow, indicating a high degree of convergence in production profiles. This narrowing of the power output spectrum implies that the optimisation process identifies a specific temporal and energetic moment as desirable. In particular, the optimiser tends to select WEC configurations whose energy production aligns with such recurring high-value wave events, favouring concentration of generation during these optimal periods rather than uniform output across the year.
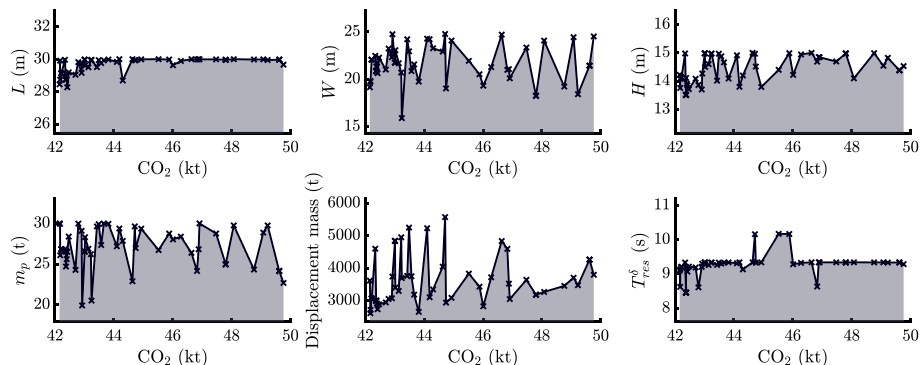


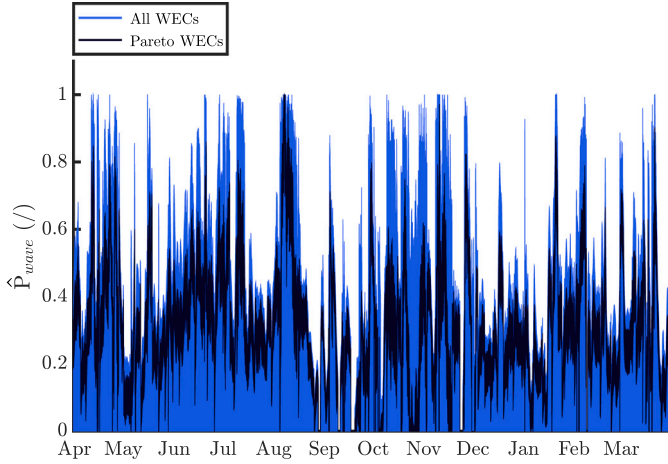**Fig. 21.** Main design parameters trend for the Pareto set WECs.

**Fig. 22.** Stripe of variation for the overall WECs design evaluated during the exploration (in blue) concerning the Pareto set one (in black).



**Fig. 23.** D1, D2 and D3 operative curves heatmap.

**Table 5**

Focus on the comparison among three devices: the device with maximum AEP among the overall investigated systems (D1), the one with the minimal CoE (D2), and a device chosen within the Pareto set (D3).

| Device | $L$ (m) | $W$ (m) | $H$ (m) | $Dr$ (m) | $m_p$ (t) | $T_{res}^{\Delta}$ (s) | $U_y$ (GWh/y) | $CO_2$ (kt) |
|---|---|---|---|---|---|---|---|---|
| D1 | 27.7 | 20.0 | 13.8 | 8.2 | 30.0 | 8.9 | 63.4 | 43.7 |
| D2 | 21.6 | 21.9 | 10.3 | 5.3 | 29.7 | 7.9 | 83.7 | 48.2 |
| D3 | 29.7 | 24.5 | 14.5 | 8.0 | 22.7 | 9.3 | 3.2 | 49.7 |

To remark the impact of the proposed co-design approach, in Table 5 three different significative systems are compared: the device with maximum AEP among the overall investigated systems (D1), the one with the minimal CoE (D2), and a device chosen within the Pareto set (D3).

Across the listed key descriptors, the designs display clear trade-offs. D1 couples the largest hull and heaviest pendulum with an 8.9 s resonance to enhance its AEP. D2 attains the minimum CoE through a shorter yet broader hull and a tuned 7.9 s period. Conversely, the Pareto-optimal D3 adopts a lightweight (*i.e.* lighter pendulum mass among the three designs) enlarged envelope and an extended 9.3 s period, reducing the RES–PP mismatch and balancing emissions.

Fig. 23 reports the operating-state heat maps of the three converters. Each map is arranged as a day–hour matrix, where columns correspond to the calendar day and rows to the hour of the day. The colour of each cell encodes the fraction of time the device is actively generating power. The maps reveal markedly different utilisation patterns. In particular, device D3 delivers a more continuous and high output throughout the year, remaining operative even in seasons when D1 and D2 are less productive.

These outcomes remark the capacity of the proposed co-design framework to tailor and tune the WECs geometry and dynamics to system-level objectives, favouring configurations whose production profiles coincide with periods of necessity, *i.e.* increasing the value of the produced wave energy.

The results presented above not only identify Pareto-optimal configurations for the La Gomera energy system but also provide relevant insights into their engineering implications. In particular, the optimisation process demonstrates that the inclusion of wave energy capacity consistently improves the system performance, even when the algorithm is free to exclude WEC installations. This outcome suggests that WECs can play a structurally beneficial role in supporting decarbonisation strategies, beyond their direct energy yield.

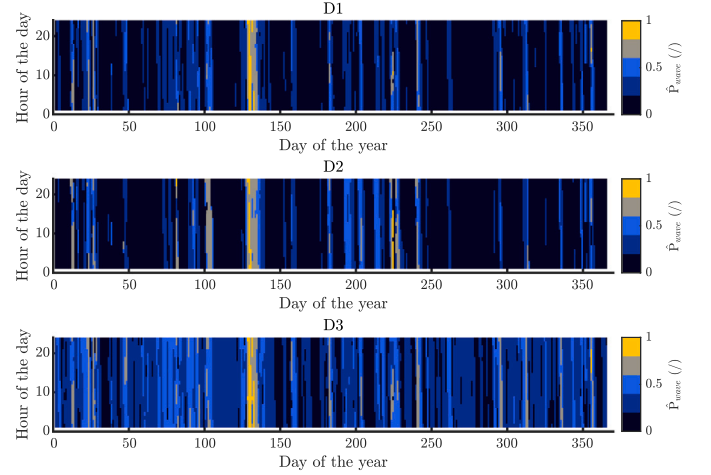A key insight is that the highest-performing WEC designs are not necessarily those maximising annual energy production, but rather those whose generation profiles are temporally aligned with demand and complementary to other RES [51,54]. This indicates that future WEC design processes should prioritise production timing and synergy with the overall energy mix, rather than focusing solely on maximising capacity factors. Such an approach could reduce the need for expensive storage capacity and minimise curtailment, ultimately improving system-level cost-effectiveness.

From an engineering standpoint, the proposed approach demonstrates its capability to highlights a practical design targets for WEC developers aiming at grid-integrated applications. Moreover, the observed narrowing of the power output distributions for Pareto-optimal devices implies that the optimiser is identifying a preferred production regime, which can guide future control strategies and tuning of the devices.

## 5. Conclusions and future works

### 5.1. Conclusions

This study introduces a novel energy system co-design framework that integrates WEC design with energy system planning, demonstrated on the PeWEC device for the La Gomera case study. By combining a multi-objective GA with EnergyPLAN simulations, the framework simultaneously optimises WEC design parameters and the energy system configuration, explicitly considering $CO_2$ reduction and RES curtailment.

Results show that wave energy capacity is consistently included in the Pareto-optimal set, confirming its positive systemic contribution under the considered resource and system conditions, despite the optimiser being allowed to install zero WEC capacity. Moreover, the best WECs systems are not necessarily those with the highest AEP but rather those whose generation profiles are temporally aligned with system demand contextually to a productive synergy with other RES, thereby reducing mismatch and storage needs. Therefore, these aspects become a fundamental criterion for the design of WEC devices, supporting greater RES penetration while minimising storage requirements and mismatch between demand and RES production. From a design perspective, optimal solutions converge around a hull length of ~30 m and a pitch resonance period of ~9 s, highlighting a preference for tuning to the most frequent wave periods rather than peak energy events. Furthermore, the wave power output curves of optimal designs set (*i.e* the Pareto devices) demonstrate a significantly narrow band compared to the wider design space, underscoring a targeted response pattern by the optimiser towards WECs designs that are effectively tuned to match specific temporal characteristics of wave energy availability. The methodology

enables significant system-wide decarbonisation, achieving up to 53 % $CO_2$ emission reduction and roughly halving the required PP capacity compared to the baseline.

The findings of the proposed sytem-aware optimisation framework highlight the potential value of the produced wave energy beyond traditional techno-economic metrics, emphasising its role in enhancing energy mix flexibility and system decarbonisation. Generally, the results demonstrate not only the technical feasibility but also the strategic relevance of co-design approaches for emerging marine renewable technologies. The methodology could serve as a reference model for integrating novel WEC technologies into energy systems, supporting decision-making processes that prioritise system-level performance.

Overall, the results validate the relevance and utility of an energy system-informed optimisation framework for WEC design, particularly in the context of high-RES island energy systems. Furthermore, this work aims to advance a methodological shift by introducing a co-design framework for WEC optimisation, in which the design process is informed not only by grid conditions but also by a bidirectional exchange of information, *i.e.* linking the behaviour of the WEC to that one of the energy system and vice versa.

Beyond the specific case study, the proposed co-design optimisation framework is generalisable to other geographies and microgrid contexts, *e.g.* remote mainland regions, hybrid off-grid communities, or interconnected but weakly supported grids. Its modular structure and energy-system-aware logic make the framework readily transferable not only to other WEC archetypes but also to emerging RES technologies. It offers a systematic approach to evaluate technology design based on system-level performance rather than isolated system's metrics, positioning the methodology as a versatile tool to support decision-making in the broader energy transition landscape.

Moreover, by directly linking technology design with energy system objectives such as $CO_2$ reduction and curtailment minimisation, the framework offers a strong basis for informing policy decisions, energy planning processes, and investment prioritisation.

### 5.2. Limitations and future works

Despite its contributions, the proposed framework is subject to several limitations that suggest paths for future research. First, the optimisation framework relies on deterministic simulations and fixed hourly demand and resource profiles. In real-world scenarios, renewable energy resource variability and forecasting are prone to different levels of uncertainty conditions that can significantly impact system performance. Incorporating stochastic or robust optimisation techniques would enhance the reliability of the proposed designs under uncertain conditions.

Second, the demand-side assumptions do not yet account for sectoral demand fluctuations, load shifting potential, or flexible consumption profiles. Integrating demand-side management and more granular sectoral models (*e.g.*, smart grids, electrified transport, desalination) would offer a more complete assessment of system performance.

The WEC model adopted in this work relies on a linear frequency-domain formulation, which (despite its efficiency and suitability for early-stage design) does not capture certain nonlinear or time-dependent interactions with the energy system. Future developments could incorporate higher-fidelity, nonlinear time-domain models to improve performance accuracy and enable the evaluation of advanced control strategies, especially under transient conditions or high-resolution simulations. This would enhance the realism and robustness of the co-design framework.

Moreover, although the model assumes a fixed BESS capacity, future work could explore dynamic BESS sizing and control strategies, including hybrid storage technologies. This extension could partially substitute the role of wave energy capacity in achieving low levels of $U_y$, but would require the introduction of efficiency or cost-related constraints to avoid unrealistic over-sizing of storage. Regulatory, financial, and social acceptance aspects were not within the scope of this work but are crucial to the real-world implementation of wave energy technologies.

In addition, the cost of WEC technology remains a key barrier to its commercial deployment and represents an important limitation of the present work, as the current framework does not directly optimise for economic metrics. It is expected that, by directly considering economic or techno-economic objective functions, the optimiser could reduce the amount of wave energy installed capacity, as it is currently much more expensive than the already industrialised technologies involved. However, since the technology investigated is still at an early stage of development, introducing cost-based constraints or objectives would be premature. Such a choice would risk overshadowing the systemic value that the integration of wave energy brings to the energy system, which the present results have highlighted as significant. In fact, the optimiser consistently selects optimal configurations with a relevant amount of installed wave energy capacity (see Fig. 20), confirming its positive contribution to system-level objectives.

Nonetheless, including economic considerations would provide a more comprehensive view. As part of future work, it is possible to extend the framework towards a three-objective optimisation problem including an energy-system level cost metric. This extension would be particularly meaningful for technologies with higher TRL, for which cost and performance indicators are more robustly defined. Such an approach would enable a balanced evaluation of techno-economic feasibility and systemic value, supporting more informed deployment strategies.

Finally, while La Gomera provides a relevant case study, further validation on larger island systems or continental microgrids would help establish the scalability and adaptability of the proposed framework across different energy transition contexts.

### CRediT authorship contribution statement

**Filippo Giorcelli:** Writing – review & editing, Writing – original draft, Visualization, Validation, Software, Methodology, Investigation, Formal analysis, Data curation, Conceptualization. **Pedro Cabrera:** Writing – review & editing, Writing – original draft, Supervision, Software, Project administration, Methodology, Investigation, Formal analysis, Conceptualization. **Bruno Paduano:** Writing – review & editing, Writing – original draft, Visualization, Supervision, Methodology, Investigation, Formal analysis. **Sergej Antonello Sirigu:** Writing – review & editing, Writing – original draft, Supervision, Software, Resources, Project administration, Methodology, Investigation, Formal analysis, Conceptualization. **Giuliana Mattiazzo:** Writing – review & editing, Supervision, Resources, Project administration, Funding acquisition.

### Declaration of competing interest

The authors declare the following financial interests/personal relationships that may be considered as potential competing interests:

Filippo Giorcelli reports that financial support was provided by Ministry of University and Research. If there are other authors, they declare that they have no known competing financial interests or personal relationships that could have appeared to influence the work reported in this paper.

### Acknowledgement

### Data availability

Data will be made available on request.

# References

[1] European Commission and Directorate-General for Research and Innovation. Horizon Europe, budget – Horizon Europe – the most ambitious EU research & innovation programme ever. Publications Office of the European Union; 2021. https://doi.org/10.2777/202859.

[2] Cabrera P, Carta JA, Gonzalez J, Melian G. Wind-driven SWRO desalination prototype with and without batteries: a performance simulation using machine learning models. Desalination 2018;435:77–96.

[3] Lund H. Renewable energy systems: a smart energy systems approach to the choice and modeling of fully decarbonized societies. Elsevier; 2024.

[4] IRENA. Off-grid renewable energy solutions to expand electricity access: an opportunity not to be missed. https://www.irena.org/publications/2019/Jan/Off-grid-renewable-energy-solutions-to-expand-electricity-to-access-An-opportunity-not-to-be-missed.

[5] IRENA. Off-grid renewable energy systems: status and methodological issues. https://www.irena.org/Publications/2015/Feb/Off-grid-renewable-energy-systems-Status-and-methodological-issues.

[6] Connolly D, Lund H, Mathiesen BV. Smart energy Europe: the technical and economic impact of one potential 100 % renewable energy scenario for the European Union. Renew Sustain Energy Rev 2016;60:1634–53.

[7] Giglio E, Fioriti D, Chihota MJ, Poli D, Bekker B, Mattiazzo G. Integrated stochastic reserve estimation and MILP energy planning for high renewable penetration: application to 2050 South African energy system. Sustain Energy Grids Netw 2025;42:101650.

[8] IRENA. 100% renewable energy scenarios: supporting ambitious policy targets. https://www.irena.org/Publications/2024/Mar/100pc-renewable-energy-scenarios-Supporting-ambitious-policy-targets.

[9] Østergaard PA, Lund H, Thellufsen JZ, Sorknaes P, Mathiesen BV. Review and validation of energyPLAN. Renew Sustain Energy Rev 2022;168:112724.

[10] Connolly D, Lund H, Mathiesen BV, Leahy M. A review of computer tools for analysing the integration of renewable energy into various energy systems. Appl Energy 2010;87(4):1059–82.

[11] Meschede H, Child M, Breyer C. Assessment of sustainable energy system configuration for a small Canary Island in 2030. Energy Convers Manag 2018;165:363–72.

[12] Cross S, Padfield D, Ant-Wuorinen R, King P, Syri S. Benchmarking island power systems: results, challenges, and solutions for long term sustainability. Renew Sustain Energy Rev 2017;80:1269–91.

[13] European Commission. Clean energy for EU islands. https://clean-energy-islands.ec.europa.eu/.

[14] European Commission. EUROISLANDS – the development of the islands – European islands and cohesion policy. https://archive.espon.eu/programme/projects/espon-2013/targeted-analyses/euroislands-development-islands-%E2%80%93-european-islands.

[15] European Commission. ISLENET: European islands energy and environment network. https://cordis.europa.eu/article/id/3632-islenet-european-islands-energy-and-environment-network.

[16] Giglio E, Luzzani G, Terranova V, Trivigno G, Niccolai A, Grimaccia F. An efficient artificial intelligence energy management system for urban building integrating photovoltaic and storage. IEEE Access 2023;11:18673–88.

[17] Colmenar-Santos A, Linares-Mena A-R, Molina-Ibáñez E-L, Rosales-Asensio E, Borge-Diez D. Technical challenges for the optimum penetration of grid-connected photovoltaic systems: Spain as a case study. Renew Energy 2020;145:2296–305.

[18] Rosales-Asensio E, Diez DB, Sarmento P. Electricity balancing challenges for markets with high variable renewable generation. Renew Sustain Energy Rev 2024;189:113918.

[19] Marocco P, Ferrero D, Lanzini A, Santarelli M. The role of hydrogen in the optimal design of off-grid hybrid renewable energy systems. J Energy Storage 2022;46:103893.

[20] Rosales-Asensio E, de Simón-Martín M, Borge-Diez D, Blanes-Peiró JJ, Colmenar-Santos A. Microgrids with energy storage systems as a means to increase power resilience: an application to office buildings. Energy 2019;172:1005–15.

[21] Mork G, Barstow S, Kabuth A, Pontes MT. Assessing the global wave energy potential. In: International conference on offshore mechanics and Arctic engineering, vol. 49118. 2010. p. 447–54.

[22] Ilyas A, Kashif SAR, Saqib MA, Asad MM. Wave electrical energy systems: implementation, challenges and environmental issues. Renew Sustain Energy Rev 2014;40:260–8.

[23] Guo B, Ringwood JV. A review of wave energy technology from a research and commercial perspective. IET Renew Power Gener 2021;15(14):3065–90.

[24] López I, Andreu J, Ceballos S, De Alegría IM, Kortabarria I. Review of wave energy technologies and the necessary power-equipment. Renew Sustain Energy Rev 2013;27:413–34.

[25] Pelc R, Fujita RM. Renewable energy from the ocean. Mar Policy 2002;26(6):471–9.

[26] Fusco F, Nolan G, Ringwood JV. Variability reduction through optimal combination of wind/wave resources–an Irish case study. Energy 2010;35(1):314–25.

[27] Pérez-Collazo C, Greaves D, Iglesias G. A review of combined wave and offshore wind energy. Renew Sustain Energy Rev 2015;42:141–53.

[28] Widén J, Carpman N, Castellucci V, Lingfors D, Olauson J, Remouit F, Bergkvist M, Grabbe M, Waters R. Variability assessment and forecasting of renewables: a review for solar, wind, wave and tidal resources. Renew Sustain Energy Rev 2015;44:356–75.

[29] Kalogeri C, Galanis G, Spyrou C, Diamantis D, Baladima F, Koukoula M, Kallos G. Assessing the European offshore wind and wave energy resource for combined exploitation. Renew Energy 2017;101:244–64.

[30] Paduano B, Parrinello L, Niosi F, Dell'edera O, Sirigu SA, Faedo N, Mattiazzo G. Towards standardised design of wave energy converters: a high-fidelity modelling approach. Renew Energy 2024;224:120141.

[31] Penalba M, Ringwood JV. A high-fidelity wave-to-wire model for wave energy converters. Renew Energy 2019;134:367–78.

[32] Guo B, Ringwood JV. Geometric optimisation of wave energy conversion devices: a survey. Appl Energy 2021;297:117100.

[33] Clemente D, Rosa-Santos P, Taveira-Pinto F. On the potential synergies and applications of wave energy converters: a review. Renew Sustain Energy Rev 2021;135:110162.

[34] Clark CE, Teruel AG, DuPont B, Forehand DIM. Towards reliability-based geometry optimization of a point-absorber with PTO reliability objectives. In: 13th European wave and tidal energy conference; 2019.

[35] Garcia-Teruel A, Forehand DIM. A review of geometry optimisation of wave energy converters. Renew Sustain Energy Rev 2021;139:110593.

[36] Cordonnier J, Gorintin F, De Cagny A, Clément AH, Babarit ASEAREV. SEAREV: case study of the development of a wave energy converter. Renew Energy 2015;80:40–52.

[37] Teillant B, Costello R, Weber J, Ringwood J. Productivity and economic assessment of wave energy projects through operational simulations. Renew Energy 2012;48:220–30.

[38] Portillo JCC, Reis PF, Henriques JCC, Gato LMC, Falcão AFO. Backward bent-duct buoy or frontward bent-duct buoy? Review, assessment and optimisation. Renew Sustain Energy Rev 2019;112:353–68.

[39] Garcia-Teruel A, Forehand DIM. Manufacturability considerations in design optimisation of wave energy converters. Renew Energy 2022;187:857–73.

[40] Garcia-Teruel A, Clark CE. Reliability-based hull geometry optimisation of a point-absorber wave energy converter with power take-off structural reliability objectives. IET Renew Power Gener 2021;15(14):3255–68.

[41] Clark CE, DuPont B. Reliability-based design optimization in offshore renewable energy systems. Renew Sustain Energy Rev 2018;97:390–400.

[42] Golbaz D, Asadi R, Amini E, Mehdipour H, Nasiri M, Etaati B, Naeeni STO, Neshat M, Mirjalili S, Gandomi AH. Layout and design optimization of ocean wave energy converters: a scoping review of state-of-the-art canonical, hybrid, cooperative, and combinatorial optimization methods. Energy Rep 2022;8:15446–79.

[43] Trueworthy A, DuPont B. The wave energy converter design process: methods applied in industry and shortcomings of current practices. J Mar Sci Eng 2020;8(11):932.

[44] McCabe R, Dietrich M, Liu A, Haji M. System level techno-economic and environmental design optimization for ocean wave energy. In: International design engineering technical conferences and computers and information in engineering conference, vol. 87301. American Society of Mechanical Engineers; 2023, p. V03AT03A033.

[45] Mai T, Mowers M, Eurek K. Competitiveness metrics for electricity system technologies, Tech. rep., National Renewable Energy Lab (NREL), Golden, CO (United States); 2021.

[46] IRENA. Renewable power generation costs in 2019, https://www.irena.org/publications/2020/Jun/Renewable-Power-Costs-in-2019 [accessed: 15.May.2025].

[47] de Faria VAD, de Queiroz AR, DeCarolis JF. Optimizing offshore renewable portfolios under resource variability. Appl Energy 2022;326:120012.

[48] Coles D, Wray B, Stevens R, Crawford S, Pennock S, Miles J. Impacts of tidal stream power on energy system security: an Isle of wight case study. Appl Energy 2023;334:120686. https://doi.org/10.1016/j.apenergy.2023.120686. https://www.sciencedirect.com/science/article/pii/S0306261923000508.

[49] Blanco M, Navarro G, Najera J, Lafoz M, Sarasua JI, García H, Martínez-Lucas G, Pérez-Díaz JI, Isabel V. Wave farms integration in a 100% renewable isolated small power system - frequency stability and grid compliance analysis. Proc Eur Wave Tidal Energy Conf 2023 Sep.;15. https://doi.org/10.36688/ewtec-2023-215. https://submissions.ewtec.org/proc-ewtec/article/view/215.

[50] Giorcelli F, Giglio E, Sirigu SA, Mattiazzo G. Power grid informed techno-economic analysis of the optimal PEWEC design. Energy 2025:137708.

[51] Cairella LC, Said HA, Pasta E. On the role of wave energy in the renewable energy mix complementarity: a comparative study between Italy and Ireland. In: Proceedings of the European wave and tidal energy conference, vol. 16. 2025.

[52] Coe RG, Lavidas G, Bacelli G, Kobos PH, Neary VS. Minimizing cost in a 100% renewable electricity grid: a case study of wave energy in California. In: International conference on offshore mechanics and Arctic engineering, vol. 85932. American Society of Mechanical Engineers; 2022, p. V008T09A073.

[53] Marañon-Ledesma H, Tedeschi E. Energy storage sizing by stochastic optimization for a combined wind-wave-diesel supplied system. In: 2015 International conference on renewable energy research and applications (ICRERA); IEEE; 2015. p. 426–31.

[54] Said HA, Skiarski A, Ringwood JV. Combined renewable resource exploitation: implications for the all-island Irish electricity supply system. Energy Convers Manag X 2025;26:100992.

[55] Ringwood JV. Control co-design for wave energy systems. Appl Ocean Res 2025;158:104514. https://doi.org/10.1016/j.apor.2025.104514. https://www.sciencedirect.com/science/article/pii/S0141118725001026.

[56] Cabrera P, Carta JA. Smart renewable energy penetration strategies on islands: the case of Gran Canaria. Energy 2018;162:421–43.

[57] Cabrera P, Carta JA, Lund H, Thellufsen JZ. Large-scale optimal integration of wind and solar photovoltaic power in water-energy systems on islands. Energy Convers Manag 2021;235:113982.

[58] Lund H. 4 - the EnergyPLAN energy system analysis model. In Lund H, editor. Renewable energy systems. 3rd ed. Academic Press; 2024. pp. 51–74. https://doi.org/10.1016/B978-0-443-14137-9.00004-8. https://www.sciencedirect.com/science/article/pii/B9780443141379000048.

[59] Lund H, Mathiesen BV. Energy system analysis of 100% renewable energy systems–the case of Denmark in years 2030 and 2050. Energy 2009;34(5):524–31.

[60] Østergaard PA. Reviewing EnergyPLAN simulations and performance indicator applications in EnergyPLAN simulations. Appl Energy 2015;154:921–33.

[61] Connolly D, Lund H, Mathiesen BV, Leahy M. The first step towards a 100% renewable energy-system for Ireland. Appl Energy 2011;88(2):502–7.

[62] Energyplan - documentation, http://www.energyplan.eu/training/documentation/ [accessed: 25.Mar.2025].

[63] Energyplan - website, http://www.energyplan.eu [accessed: 25.Mar.2025].

[64] Lund H, Thellufsen JZ, Østergaard PA, Sorknaes P, Skov IR, Mathiesen BV. Energyplan–advanced analysis of smart energy systems. Smart Energy 2021;1:100007.

[65] Cabrera P, Lund H, Thellufsen JZ, Sorknaes P. The MATLAB toolbox for EnergyPLAN: a tool to extend energy planning studies. Sci Comput Program 2020;191:102405.

[66] Jiménez A, Cabrera P, Medina JF, Østergaard PA, Lund H. Smart energy system approach validated by electrical analysis for electric vehicle integration in islands. Energy Convers Manag 2024;302:118121.

[67] Red eléctrica - website, https://demanda.ree.es/visiona/seleccionar-sistema [accessed: 25.Mar.2025].

[68] Openmeteo - website, https://open-meteo.com/en/docs/historical-weather-apistart_date022-01-01&end_date2022-12-31&daily [accessed: 25.Mar.2025].

[69] Yanez-Rosales P, Del Río-Gamero B, Schallenberg-Rodríguez J. Rationale for selecting the most suitable areas for offshore wind energy farms in isolated island systems. case study: Canary Islands. Energy 2024;307:132589.

[70] Deb K, Pratap A, Agarwal S, Meyarivan TAMT. A fast and elitist multiobjective genetic algorithm: NSGA-II. IEEE Trans Evol Comput 2002;6(2):182–97.

[71] Gobierno de Canarias. BOC n. 242. Miércoles 4 de diciembre de 2024 - 4037. https://www.gobiernodecanarias.org/boc/2024/242/4037.html.

[72] Gobierno de Canarias. BOC n. 015. Jueves 23 de enero de 2025 - 302. https://www.gobiernodecanarias.org/boc/2025/015/302.html.

[73] Instituto Canario de Estadistica (ISTAC), https://www.gobiernodecanarias.org/istac/estadisticas/sectorsecundario/industria/energia/C00022A.html [accessed: 25.Mar.2025].

[74] Gobierno de Canarias, Canary Islands energy yearbooks, https://www.gobiernodecanarias.org/energia/materias/anuarios-energeticos/ [accessed: 25.Mar.2025].

[75] Dirección General de Industria y Energía del Gobierno de Canarias. Proyecto piloto sobre la caracterización de los usos finales de la energía en diferentes tipos de consumidores en Canarias. N.d.

[76] Gobierno de Canarias, Plan Director de Actuaciones en el ÁAmbito de las Áreas Industriales de Canarias (PDAIC), Isla de La Gomera, https://www.gobiernodecanarias.org/industria/PDAIC/ [accessed: 25.Mar.2025].

[77] Era5- website, https://cds.climate.copernicus.eu/datasets/reanalysis-era5-single-levels?tab=download [accessed: 25.Mar.2025].

[78] Carapellese F, Pasta E, Paduano B, Faedo N, Mattiazzo G. Intuitive LTI energy-maximising control for multi-degree of freedom wave energy converters: the PEWEC case. Ocean Eng 2022;256:111444.

[79] Dell'edera O, Niosi F, Casalone P, Bonfanti M, Paduano B, Mattiazzo G. Understanding wave energy converters dynamics: high-fidelity modeling and validation of a moored floating body. Appl Energy 2024;376:124202.

[80] Paduano B, Carapellese F, Pasta E, Sirigu SA, Faedo N, Mattiazzo G. Data-based control synthesis and performance assessment for moored wave energy conversion systems: the PEWEC case. IEEE Trans Sustain Energy 2023;15(1):355–67.

[81] Sirigu SA, Foglietta L, Giorgi G, Bonfanti M, Cervelli G, Bracco G, Mattiazzo G. Techno-economic optimisation for a wave energy converter via genetic algorithm. J Mar Sci Eng 2020;8(7):482.

[82] Giorcelli F, Sirigu SA, Pasta E, Gioia DG, Bonfanti M, Mattiazzo G. Wave energy converter optimal design under parameter uncertainty. In: International conference on offshore mechanics and Arctic engineering, vol. 85932. American Society of Mechanical Engineers; 2022, p. V008T09A085.

[83] Giglio E, Petracca E, Paduano B, Moscoloni C, Giorgi G, Sirigu SA. Estimating the cost of wave energy converters at an early design stage: a bottom-up approach. Sustainability 2023;15(8):6756.

[84] Paduano B, Carapellese F, Pasta E, Faedo N, Mattiazzo G. Optimal controller tuning for a nonlinear moored wave energy converter via non-parametric frequency-domain techniques. Trends Renew. Energ. Offshore 2022:393–400.

[85] Faedo N, Carapellese F, Pasta E, Mattiazzo G. On the principle of impedance-matching for underactuated wave energy harvesting systems. Appl Ocean Res 2022;118:102958.

[86] Pasta E, Carapellese F, Mattiazzo G. Deep neural network trained to mimic nonlinear economic model predictive control: an application to a pendulum wave energy converter. In: 2021 IEEE conference on control technology and applications (CCTA); IEEE; 2021. p. 295–300.

[87] Papini G, Pasta E, Carapellese F, Bonfanti M. Energy-maximising model predictive control for a multi degree-of-freedom pendulum-based wave energy system. IFAC-Pap. 2022;55(31):433–8.

[88] Gioia DG, Pasta E, Brandimarte P, Mattiazzo G. Data-driven control of a pendulum wave energy converter: a Gaussian process regression approach. Ocean Eng 2022;253:111191.

[89] Niosi F, Begovic E, Bertorello C, Rinauro B, Sannino G, Bonfanti M, Sirigu SA. Experimental validation of OrcaFlex-based numerical models for the PEWEC device. Ocean Eng 2023;281:114963.

[90] Pozzi N, Bracco G, Passione B, Sirigu SA, Mattiazzo G. Pewec: experimental validation of wave to PTO numerical model. Ocean Eng 2018;167:114–29.

[91] Carapellese F, Faedo N. Mechanical interactions modeling of inertial wave energy converters. Int J Mech Sci 2024;284:109731.

[92] Folley M. Numerical modelling of wave energy converters: state-of-the-art techniques for single devices and arrays. Academic Press; 2016.

[93] Faltinsen O. Sea loads on ships and offshore structures. Vol. 1. Cambridge University Press; 1993.

[94] Babarit A, Delhommeau G. Theoretical and numerical aspects of the open source BEM solver Nemoh. In: 11th European wave and tidal energy conference (EWTEC2015); 2015.

[95] Ringwood JV, Bacelli G, Fusco F. Energy-maximizing control of wave-energy converters: the development of control system technology to optimize their operation. IEEE Control Syst Mag 2014;34(5):30–55.

[96] Pasta E, Faedo N, Mattiazzo G, Ringwood JV. Towards data-driven and data-based control of wave energy systems: classification, overview, and critical assessment. Renew Sustain Energy Rev 2023;188:113877.

[97] Papini G, Faedo N, Mattiazzo G. Fault diagnosis and fault-tolerant control in wave energy: a perspective. Renew Sustain Energy Rev 2024;199:114507.

[98] Faedo N, Peña-Sanchez Y, Carapellese F, Mattiazzo G, Ringwood JV. LMI-based passivation of LTI systems with application to marine structures. IET Renew Power Gener 2021;15(14):3424–33.

[99] Bonfanti M, Sirigu SA. Spectral-domain modelling of a non-linear wave energy converter: analytical derivation and computational experiments. Mech Syst Signal Process 2023;198:110398.

[100] Pecher A, Kofoed JP. Handbook of ocean wave energy. Springer Nature; 2017.

[101] Hasselmann K, Barnett TP, Bouws E, Carlson H, Cartwright DE, Enke K, Ewing JA, Gienapp A, Hasselmann DE, Kruseman P, et al. Measurements of wind-wave growth and swell decay during the joint north sea wave project (jonswap). Ergaenzungsh. Dtsch Hydrogr Z Reihe A 1973.

[102] Chang G, Jones CA, Roberts JD, Neary VS. A comprehensive evaluation of factors affecting the levelized cost of wave energy conversion projects. Renew Energy 2018;127:344–54.

[103] Lavidas G, Blok K. Shifting wave energy perceptions: the case for wave energy converter (WEC) feasibility at milder resources. Renew Energy 2021;170:1143–55.

[104] Ocean Energy Europe. 2030 ocean energy vision, https://www.oceanenergy-europe.eu/wp-content/uploads/2020/10/OEE_2030_Ocean_Energy_Vision.pdf [accessed: 21.Nov.2024].

[105] Sandia National Laboratiries. Technological cost-reduction pathways for attenuator wave energy converters in the marine hydrokinetic environment, https://www.osti.gov/servlets/purl/1096511 [accessed: 21.Nov.2024].

[106] U. S. D. of Energy Wind & Water Power Technologies Program. The future potential of wave power in the United States, https://www.ourenergypolicy.org/wp-content/uploads/2012/10/The-Future-of-Wave-Power-MP-9-20-12.pdf [accessed: 21.Nov.2024].

[107] MacGillivray A, Jeffrey H, Winskel M, Bryden I. Innovation and cost reduction for marine renewable energy: a learning investment sensitivity analysis. Technol Forecast Soc Change 2014;87:108–24.

[108] Etri EC. Energy technology reference indicator projections for 2010–2050. Joint research centre (JRC), European Commission (EC) 2014.

[109] Ringwood JV, Zhan S, Faedo N. Empowering wave energy with control technology: possibilities and pitfalls. Annu Rev Control 2023;55:18–44.

[110] Guanche R, De Andres AD, Simal PD, Vidal C, Losada IJ. Uncertainty analysis of wave energy farms financial indicators. Renew Energy 2014;68:570–80.

[111] De Andres A, Medina-Lopez E, Crooks D, Roberts O, Jeffrey H. On the reversed LCOE calculation: design constraints for wave energy commercialization. Int J Mar Energy 2017;18:88–108.

[112] Ambühl S, Marquis L, Kofoed JP, Dalsgaard Sørensen J. Operation and maintenance strategies for wave energy converters. Proc Inst Mech Eng Part O J Risk Reliab 2015;229(5):417–41.

[113] Guanche R, De Andrés A, Losada IJ, Vidal C. A global analysis of the operation and maintenance role on the placing of wave energy farms. Energy Convers Manag 2015;106:440–56.

[114] De Andres A, Maillet J, Hals Todalshaug J, Möller P, Bould D, Jeffrey H. Techno-economic related metrics for a wave energy converters feasibility assessment. Sustainability 2016;8(11):1109.

[115] O'Connor M, Lewis T, Dalton G. Operational expenditure costs for wave energy projects and impacts on financial returns. Renew Energy 2013;50:1119–31.

[116] Red Eléctrica. Tenerife-La Gomera link. https://www.ree.es/es/transporte-electricidad/proyectos-transporte/proyecto-tenerife-gomera.